Comparative Industrial-Scale Life Cycle Assessment of Base Case and Heat Recovery Scenarios for Carbon Capture from Natural Gas Combined Cycle power plants using Aqueous Ammonia

Pancy Ang[a,*], Wayne Goh[a], Jie Bu[a], Shuying Cheng[a,*]

[a] Institute of Sustainability for Chemicals, Energy and Environment (ISCE^2), Agency for Science, Technology and Research (A*STAR), 1 Pesek Road, Singapore 627833, Republic of Singapore

*Corresponding Authors: pancy_ang@isce2.a-star.edu.sg and cheng_shuying@isce2.a-star.edu.sg.

ABSTRACT

As social and economic activities return to pre-COVID-19 levels, greenhouse gas emissions continue to rise, exacerbating climate change. This study explores carbon capture and sequestration (CCS) technologies to mitigate carbon dioxide (CO_2) emissions from Natural Gas Combined Cycle (NGCC) power plants, proposing aqueous ammonia as a solvent due to its high reactivity and lower energy regeneration requirements. A life cycle assessment (LCA) was conducted to compare a base case with a heat recovery scenario for capturing 300 kilotonnes of CO_2 annually from NGCC flue gas. The cradle-to-gate LCA, using a functional unit of one tonne of CO_2 input, encompasses the process from flue gas extraction to the production of purified CO_2. The heat recovery scenario outperformed the base case in all environmental impact categories. The LCA results indicated a net carbon abatement of 94.49 kg CO_2 eq. for the base case and 508.69 kg CO_2 eq. for the heat recovery scenario. Key contributors to global warming potential (GWP) included electricity consumption and heat production, while human toxicity potential (HTP) and marine aquatic ecotoxicity potential (MAETP) were significant environmental impact categories. Sensitivity analysis and Monte Carlo simulation highlighted critical parameters and uncertainties, and scenario analysis examined additional variables for a comprehensive assessment. Aqueous ammonia not only lowers emissions but also provides cost-effectiveness and high absorption efficiency, positioning it as a viable option for large-scale CO_2 capture. Additionally, it has the potential for future integration with the carbonation of municipal and industrial solid waste, contributing to sustainable waste management and carbon sequestration.

KEYWORDS: life cycle assessment, carbon capture, aqueous ammonia, industrial scale, natural gas combined cycle, heat recovery

INTRODUCTION

Both social and economic activities have begun to return to levels preceding the COVID-19 pandemic, while the climate continues to respond to the ongoing increase in greenhouse gases and resulting warming. Over the past 800,000 years, atmospheric carbon dioxide (CO_2) levels remained below 300 ppm, but in the last 60 years, human-induced increases have occurred 100 times faster than natural changes based on data from Lüthi, et al., 2008.[1] The largest source of CO_2 emissions from human activities in Europe (EU), China, and the Asia-Pacific region is from electricity and heat producers, accounting for 49%, 56%, and 53% of total CO_2 emissions, respectively.[2-4] With growing concern over climate change and the increasing need to reduce greenhouse gas emissions, carbon capture and sequestration (CCS) has emerged as a crucial technology for mitigating carbon emissions from existing fossil fuel-based power plants.[5-8] This process involves capturing CO_2 from the flue gas emitted after the combustion of fossil fuels, primarily in power generation.

Natural Gas Combined Cycle (NGCC) technology is crucial in reducing CO_2 emissions. NGCC plants emit approximately 50% less CO_2 compared to coal-fired plants and 30% less compared to oil-fired plants due to their higher efficiency and the cleaner combustion properties of natural gas. Additionally, the lower levels of impurities such as hydrogen sulfide, sulfur oxides, nitrogen oxides, and hydrochloric acid in natural gas simplify the CCS process and reduce associated costs. NGCC power plants are widely adopted for electricity generation in regions like the United States (U.S.) and EU due to their efficiency in utilizing natural gas as a fuel source. Coal combustion accounted for 55% of CO_2 emissions but only 20% of U.S. electricity in 2022, while natural gas, the largest source, contributed about 40%.[9] Singapore (SG) made early policy choices that reduced the

greenhouse gas emissions by switching from fuel oil to natural gas for power generation. In 2022, about 92% of its electricity was generated from natural gas, compared to 18% in 2000.[10]

The CO_2 concentration in the flue gas from NGCC power plants is about 3% to 3.5% because of the excess air ratio required to maintain optimal temperatures in the gas turbines.[11] This excess air dilutes the CO_2 concentration in the exhaust gases. Since the combustion process uses a large amount of air, the resulting flue gas is mostly nitrogen and water vapor, with CO_2 constituting only a small fraction. This low concentration presents challenges for CO_2 capture, as the capture process becomes more complex and energy-intensive due to the need to separate CO_2 from the large volume of flue gas primarily composed of non-condensable gases.[12]

There are three primary methods of CO_2 capture: post-combustion capture, oxy-fuel combustion, and pre-combustion capture.[13] [14] Oxy-fuel combustion, where fossil fuels is combusted in a mixture of oxygen and recycled flue gas instead of air, produces a flue gas that is primarily CO_2 and water vapor, which can be easily separated by cooling and condensing the water vapor, leaving nearly pure CO_2. While this method provides a high concentration of CO_2 in the flue gas, it requires an air separation unit to produce oxygen, which can be energy-intensive and costly.[15-17] Pre-combustion capture involves converting fossil fuels into a mixture of hydrogen and CO_2 before combustion. This method is typically applied in integrated gasification combined cycle (IGCC) plants, where coal or natural gas is gasified to produce syngas. Although pre-combustion capture can achieve high CO_2 capture rates, it requires significant modifications to the power plant and is more complex compared to post-combustion capture.[16, 17]

Among these methods, post-combustion capture is the most applicable for NGCC power plants due to its ability to be integrated with existing infrastructure with minimal modifications.[18] This flexibility makes it particularly attractive for retrofitting existing power plants, allowing for a quicker and more cost-effective implementation. Additionally, post-combustion capture technology is well-established and has been extensively studied and optimized, providing a reliable solution for immediate CO_2 reduction needs.[15-17] Post-combustion capture removes CO_2 from the flue gas emitted after the combustion of fossil fuels. This process operates at low CO_2 concentrations (10–20 vol%) and ambient pressure, using amine-based chemical absorbents, such as monoethanolamine (MEA), diethanolamine, N-methyldiethanolamine and piperazine, in aqueous solutions.[19-24]

MEA-based post-combustion chemical absorption is currently the most viable technology for carbon capture from fossil fuel power plants, utilizing MEA as an established solvent for CO_2 separation from flue gas. However, it demands substantial thermal energy for solvent regeneration in the stripper.[18] This method is more suitable for coal-fired power plants and less effective for NGCC power plants due to the lower CO_2 concentration (4%) in their flue gas. Nonetheless, process and solvent optimization can reduce energy consumption to 0.2 MWh per ton of CO_2.[25] Integrating an NGCC power plant with a post-combustion capture process incurs an energy penalty, decreasing the net thermal efficiency of the NGCC from 58.5% to 50.6%.[26] Additionally, MEA is prone to degradation and corrosion, requiring frequent solvent replacement, which further increases maintenance costs.[27]

In contrast, ammonia-based CO_2 capture has gained attention as a promising alternative. Ammonia offers several advantages over MEA, particularly its lower

regeneration temperature, which can reduce thermal energy consumption by up to 27–33%.[27, 28] Additionally, ammonia has a higher CO_2 capture capacity, up to 1 mol of CO_2 per mol of ammonia, compared to MEA's 0.5 mol of CO_2 per mol of MEA, and is less prone to degradation and corrosion, extending the solvent's lifespan and reducing operational costs.[27, 28] A potential advantage of ammonia-based systems is their ability to integrate with industrial waste carbonation processes.[29] Once CO_2 is captured in the ammonia solution, it can be used to carbonate alkaline industrial wastes, such as steel slag, fly ash, and construction debris. This carbonation process converts CO_2 into stable mineral carbonates, like calcium carbonate, providing dual benefits: reducing atmospheric CO_2 and minimizing industrial waste.[29]

Ammonia-based CO_2 capture systems are already being tested and implemented at both pilot and industrial scales. For example, Alstom's Chilled Ammonia Process (CAP) has shown promising results, capturing over 90% of CO_2 in pilot projects at power plants such as the Mountaineer Plant in the U.S.[27] Similarly, the CSIRO ammonia-based process in Australia has demonstrated a 90% CO_2 capture efficiency, with a product purity exceeding 99%.[30] These pilot projects highlight the significant potential of ammonia-based CO_2 capture systems for widespread industrial application, particularly in sectors like power generation, cement production, and steel manufacturing, where large amounts of CO_2 and alkaline waste are generated. This presents an opportunity for effective integration of ammonia-based capture technologies. Building on these pilot study results, ammonia-based CO_2 capture systems can be further optimized for commercial-scale deployment, particularly when combined with industrial waste carbonation processes. Ammonia offers

an efficient method for CO_2 sequestration while also providing a viable solution for future industrial waste management.

This study focuses on the life cycle assessment (LCA) of the absorption and desorption processes to evaluate the feasibility of integrating this technology with carbonation and other subsequent processes. Our process involves CO_2 absorption to form ammonium bicarbonate and ammonium carbonate, which can then be decomposed to release pure CO_2 for storage or utilization. However, a significant challenge in this process is ammonia slip, where NH_3 escapes from the absorber along with the treated flue gas, posing both environmental and operational risks. Mitigation strategies such as washing stages and additional absorption units are essential to address this issue.[31] Extensive research has been conducted to understand the fundamental aspects of post-combustion CO_2 capture by aqueous ammonia, focusing on the chemical reaction processes, factors influencing these reactions (including ammonia and CO_2 concentrations, flow rates, and temperature), and methods to enhance absorption.[32-34] Despite these challenges, ammonia-based CO_2 capture offers several advantages, including low cost, high absorption efficiency, and high absorption capacity, making it a viable and attractive option for large-scale CO_2 capture.[35]

The high-purity CO_2 product has numerous current and potential applications. Present uses include the food and beverage industry, geological sequestration, enhanced oil recovery, and medical applications.[36-39] Additionally, converting CO_2 into chemicals such as urea, formic acid, and organic carbonates, like ethylene carbonates, presents a high-value market opportunity, potentially sequestering around 500 Mt of CO_2 annually.[40, 41] Talita et al. discuss various emerging technologies for converting CO_2 into high-value products like

methanol, ethanol and other hydrocarbons, which are in different stages of development, with technological readiness levels (TRL) ranging from 2 to 9.[42] Further research is needed to investigate and evaluate the challenges for these technologies to advance to higher TRLs.[43]

Conducting LCA on CCS using aqueous ammonia is essential for evaluating the environmental impacts of this technology across its entire life cycle. LCA helps identify key areas for improving environmental benefits and minimizing negative impacts, such as balancing energy consumption during capture with the overall reduction in greenhouse gas emissions. This thorough analysis aids in informed decision-making and the optimization of CCS systems. Strube et al. and Stefanica et al. emphasize the significance of LCA in evaluating the environmental performance and sustainability of CCS technologies employing aqueous ammonia.[44, 45]

Petrescu et al. investigated various CCS technologies, finding that while global warming potential (GWP) impacts decreased compared to the base case scenario, other impacts increased.[46] Specifically, when using aqueous ammonia as a chemical solvent, the production of ammonia, commissioning of CO_2 pipelines, and CO_2 transport and storage contributed to these increases.[46] Comparing aqueous ammonia to calcium looping for CO_2 capture, aqueous ammonia showed better performance in environmental impact categories related to lethal concentration.[46]

Matin et al. discovered that while including a CO_2 capture unit decreased GWP, it increased impacts in other categories such as ozone depletion, ionizing radiation, marine eutrophication, smog, and fossil fuel depletion.[47] Ammonia-based CO_2 capture offers

benefits such as low cost, no solvent degradation, low regeneration energy, and high CO_2 capacity.[47] However, it performs worse in terms of carbon and water footprints compared to MEA-based CO_2 capture.[47]

In our study, we modelled and presented two scenarios — base case and heat recovery for capturing low-concentration CO_2 from the flue gas of NGCC power plants using aqueous ammonia. These models were employed to perform an industrial-scale LCA to evaluate and compare environmental performance across various impact categories. Our LCA encompasses the entire process, from flue gas extraction at the NGCC power plant to the production of purified CO_2. Through this analysis, we identified critical hotspots associated with significant environmental impacts within the process. Furthermore, we integrated sensitivity analysis and Monte Carlo simulation to pinpoint key parameters and uncertainties, respectively. We also conducted scenario analysis to explore additional factors by varying electricity profiles and incorporating acid wash in the heat recovery process, thereby providing a comprehensive assessment of the observed environmental impacts.

MATERIALS AND METHODS

Base Case Process Description. In the base case process (Figure 1), 300 kilotonnes per year of simulated low-concentration CO_2 (3 vol%) – typical of the flue gas composition emitted from a NGCC power plant – are absorbed in a packed absorber (AB01) using an aqueous ammonia solution.[48] Aspen Plus® V14 software was used to calculate the mass balance and energy consumption of the process.[49] The flue gas is first cooled using gas cooler (HX01) and then compressed in a centrifugal compressor (C01) to facilitate flow through the system. CO_2 from the flue gas is chemically absorbed into the aqueous ammonia solution, resulting in a clean gas product free of CO_2 and a liquid product of water and compounds formed by ammonia and carbon dioxide. The liquid product is then pumped (P01), preheated and fed into a packed column known as the desorber (DSP01). In DSP01, the liquid feed is heated to separate CO_2 from the aqueous ammonia solution. This process yields a regenerated aqueous ammonia solution and a high-purity CO_2 product suitable for various applications. The liquid product from DSP01 preheats the desorption feed in the pre-heater (HX03) and is mixed with fresh aqueous ammonia before being cooled in the solvent cooler (HX02) for absorption. Several additional pieces of equipment support the main operation. A wash tower (WT01) and flash vessels (V01, V02) recover NH_3 vapors emitted during absorption and desorption.

Natural gas-fired heat is utilized for heating, and refrigerant cooling powered by electricity is employed to maintain absorption temperatures at 20°C. The process was simulated at a scale representative of a pilot-scale CO_2 capture plant.[50] The composition of the flue gas is detailed in Table S1 of the supporting information (SI). In the base case

scenario, heat recovery is restricted to a preheater that extracts heat from the reboiler in DSP01 and preheats the rich liquid stream from AB01 in preparation for desorption.

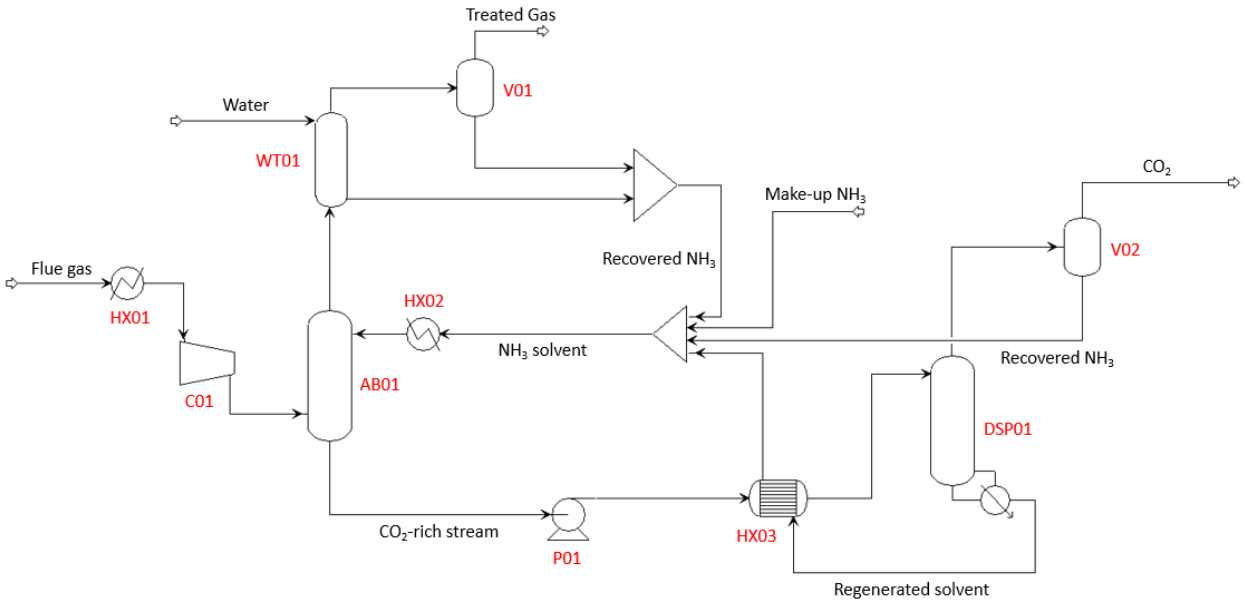

Figure 1. Schematic representation of our base case process from cradle to gate, obtained using Aspen Plus® V14.

Heat Recovery Process Description. In the heat recovery process (Figure 2), thermal energy is harnessed from various sources, such as the flue gas and liquid products from the desorption reboiler and the stripper reboiler. Adapting the design approach of Bonalumi et al., we implemented the use of a preheater to recover heat between the absorber (AB02) and the desorber (DSP02), as well as between the wash tower (WT02) and the stripper (ST01).[51] This design combines all the heat sources and sinks into a single multi-stream heat exchanger (HX06). This study assesses the efficiency and emission footprint of such an integration. The supporting equipment comprises solvent cooler (HX04) and water tank cooler (HX05), which are utilized to cool the solvents for absorption and water wash operations, respectively. Flash vessel (V03) functions similarly to flash vessel (V01) in the

base case process. The compressor (C02) and pump (P02) perform the same functions as the previously mentioned C01 and P01. All other operating conditions and inputs remain unchanged. As with the Base Case process, Aspen Plus® V14 software was utilized.[49]

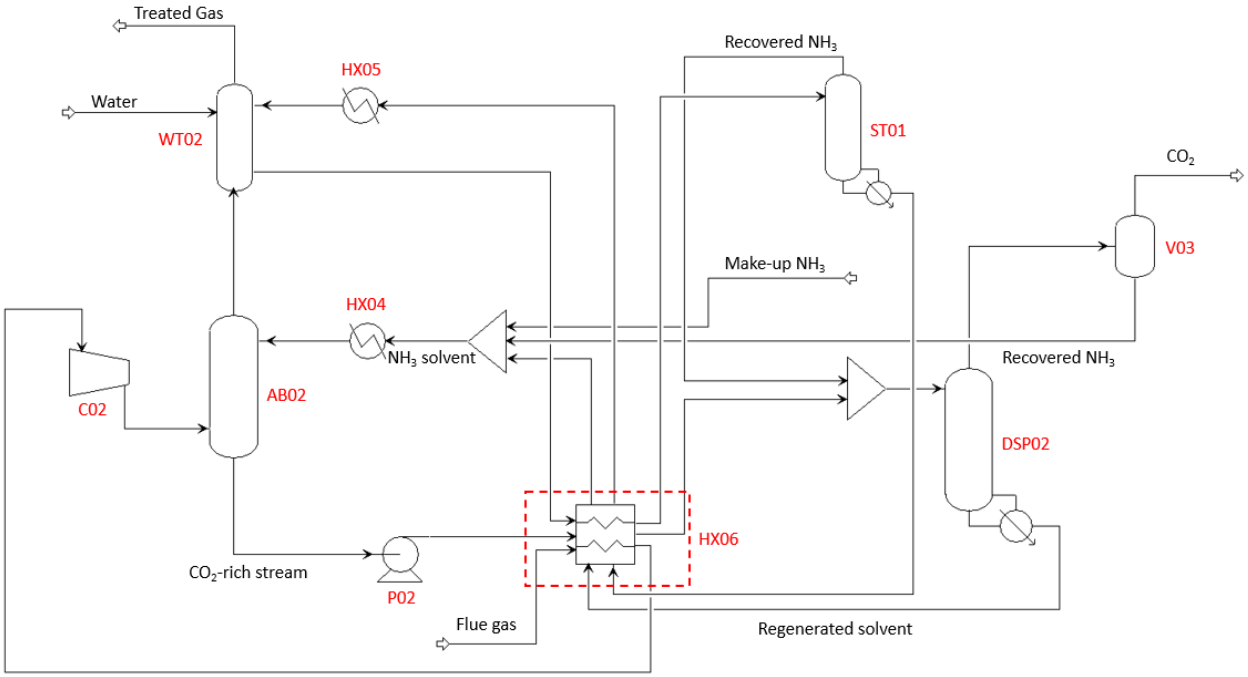

Figure 2. Schematic representation of our heat recovery process from cradle to gate, obtained using Aspen Plus® V14.

LCA Methodology. The LCA methodology in our study is based on the principles and frameworks of ISO 14040[52] and further supported by the requirements and guidelines of ISO 14044.[53] Adhering to these standards ensures the consistency, comparability, credibility, and reliability of our LCA. The methodology comprises four sequential steps: (1) goal and scope definition, (2) inventory analysis, (3) impact assessment, and (4) results interpretation.

Goal and scope definition. The goal of the LCA is to assess and compare the environmental impacts of the carbon capture process per tonne of CO_2 input for both the

base case and the heat recovery process. The scope of the LCA establishes the boundaries, context, and specific parameters that will direct the entire study. A "cradle-to-gate" system boundary is used, as illustrated in Figure 1, and the model is developed using Sphera® LCA for Experts (GaBi) version 10.8.0.14 software.[54] Detailed LCA models for both the base case and heat recovery processes are presented in the SI as Figures S1 and S2, respectively.

Before initiating an LCA study, it is essential to establish the modeling parameters. Both the base case and heat recovery processes begin with the utilization of incineration flue gas from an NGCC power plant, using one tonne of CO_2 input as the functional unit, and conclude with the production of purified CO_2. The calculation of resource and energy consumption, along with their associated emissions, is based on mass allocation. The cut-off criterion is set at 0.10% of the reference flow, and all electricity requirements are met by the SG national electricity grid, which consists of natural gas (94.3%), petroleum products (0.3%), coal (0.9%), and other sources (4.4%).[55] This data reflects the fuel mix for SG's electricity generation as of June 2023, with the 0.3% of petroleum products divided between diesel (0.15%) and fuel oil (0.15%), and the 4.4% from other sources assumed to be entirely derived from waste-to-energy. The thermal energy required for both processes is generated using an industrial furnace that utilizes natural gas as the primary fossil fuel source.

Inventory analysis. The Life Cycle Inventory (LCI) process is the second step in LCA, involving the compilation and quantification of inputs and outputs for a product system throughout its life cycle. This encompasses data on materials, energy, water usage, and emissions to air, water, and soil. The LCI phase is crucial as it provides the detailed data necessary for a comprehensive and accurate LCA to assess environmental impacts effectively. LCA modeling necessitates the

careful selection of relevant data from Ecoinvent v3.9.1, as detailed in Table S5 of the SI.[56] Input-output data for both the base case and the heat recovery processes are obtained from the stream results generated by our simulation model in Aspen Plus® V14, with detailed information provided in Tables S2 and S3 of the SI.[49] The LCI analysis for the environmental profile of electricity generation in SG for June 2023 follows the methodology described by Tan et al.[57] This analysis includes the calculation and incorporation of cradle-to-gate air emissions for generating 1 MWh of electricity delivered to the national grid, accounting for a 2.5% transmission loss. The specific details of this LCI are presented in Table S4 of the SI and have been used in our previous work.[29]

Impact Assessment. The CML 2001 – Aug. 2016 life cycle impact assessment (LCIA) methodology is chosen for impact assessment in our work. Firstly, it is widely used in LCA studies, particularly for post-combustion CO_2 technologies, indicating its relevance and applicability to similar research contexts.[58-60] Additionally, it is classified as a midpoint method, offering advantages such as simplified complexity, ease of quantification, data availability, scientific basis, consistency, and interpretability.[61] Furthermore, the methodology provides a thorough assessment of environmental impacts and offers transparency and clarity in its approach, facilitating comprehension and interpretation of results.[61] Its reputation as a well-established and renowned methodology underscores its rigour and comprehensiveness, making it a reliable choice for impact assessment. Lastly, its compatibility with widely used LCA software, such as Sphera® LCA for Experts (GaBi), ensures seamless integration into research workflows, enhancing efficiency and accuracy.[54]

RESULTS AND DISCUSSIONS

Life Cycle Assessment. The LCA performance for the base case and heat recovery processes are evaluated by analyzing the cradle-to-gate impacts per tonne of carbon dioxide input. The eight selected environmental impact categories include global warming potential (kg CO_2 eq.), acidification potential (kg SO_2 eq.), eutrophication potential (kg PO_4 eq.), freshwater aquatic ecotoxicity potential (kg DCB eq.), human toxicity potential (kg DCB eq.), marine aquatic ecotoxicity (kg DCB eq.), photochemical ozone creation potential (kg C_2H_4 eq.), and terrestrial ecotoxicity potential (kg DCB eq.). Abiotic depletion potential of elements, abiotic depletion potential of fossil fuels, and ozone layer depletion are excluded, as they do not contribute to environmental impacts in this context. The impacts are calculated automatically from the inventory analysis results using Sphera® LCA for Experts (GaBi) version 10.8.0.14 software, which integrates characterization factors from CML2001 – Aug. 2016.[54, 62]

Global Warming Potential. According to Figure 3, the base case scenario's greatest impact on Global Warming Potential (GWP) is primarily due to electricity consumption, which accounts for 355.92 kg CO_2 eq. (50.45%). This is followed by heat production at 348.53 kg CO_2 eq. (49.40%), natural gas production at 0.73 kg CO_2 eq. (0.10%), and natural gas import from Indonesia (ID) at 0.30 kg CO_2 eq. (0.04%). In the heat recovery scenario, electricity consumption remains the largest driver at 289.14 kg CO_2 eq. (91.60%), followed by heat production at 26.42 kg CO_2 eq. (8.37%), natural gas production at 5.56×10^{-2} kg CO_2 eq. (0.02%), and natural gas import from ID at 2.26×10^{-2}kg CO_2 eq. (0.01%). CO_2 is the major contributor to GWP, followed by methane and nitrous oxide. The base case and heat recovery processes mitigate 799.97 kg CO_2 eq. and 824.28 kg CO_2 eq., respectively,

through the production of high-purity CO_2. The heat recovery scenario achieves an additional 414.63 kg CO_2 eq. reduction in GWP compared to the base case, primarily due to the implementation of a multi-stream heat exchanger, which significantly decreases the heat production requirement by a factor of 13.19. Maximizing internal heat recovery within the system boundaries reduces the need for external heat input, significantly lowering the GWP impact associated with heat production.

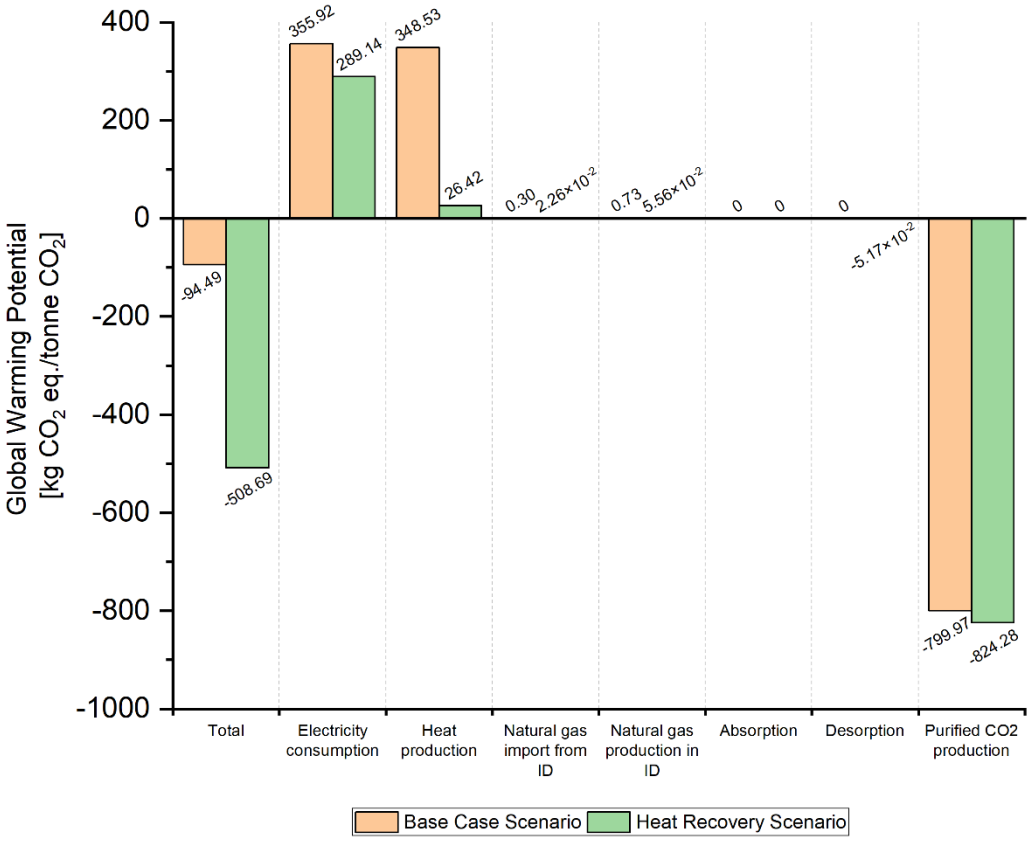

Figure 3. Global Warming Potential results for the base case and heat recovery processes, based on an input of one tonne of CO_2.

Acidification Potential. In comparing the base case and heat recovery scenarios, the base case process contributes 0.15 kg SO_2 eq. to Acidification Potential (AP), whereas the heat recovery process achieves a net positive abatement of 2.43×10^{-2} kg SO_2 eq. For both scenarios, electricity consumption is the largest source of AP (Base Case: 0.27 kg SO_2 eq.; Heat Recovery: 0.22 kg SO_2 eq.), followed by heat production (Base Case: 5.97×10^{-2} kg SO_2 eq.; Heat Recovery: 4.53×10^{-3} kg SO_2 eq.). In the base case, the absorber accounts for 4.32% of AP, and natural gas production contributes 0.25%. In the heat recovery scenario, natural gas production has a minor impact on AP, contributing 0.03%. Nitrogen oxides and sulfur dioxide contribute to AP. In both processes, nitrogen oxides are the principal pollutants, primarily emitted from electricity consumption. The production of high-purity CO_2 via the base and heat recovery processes reduces AP by 0.18 kg SO_2 eq. and 0.25 kg SO_2 eq., respectively. The AP results are presented in Figure 4.

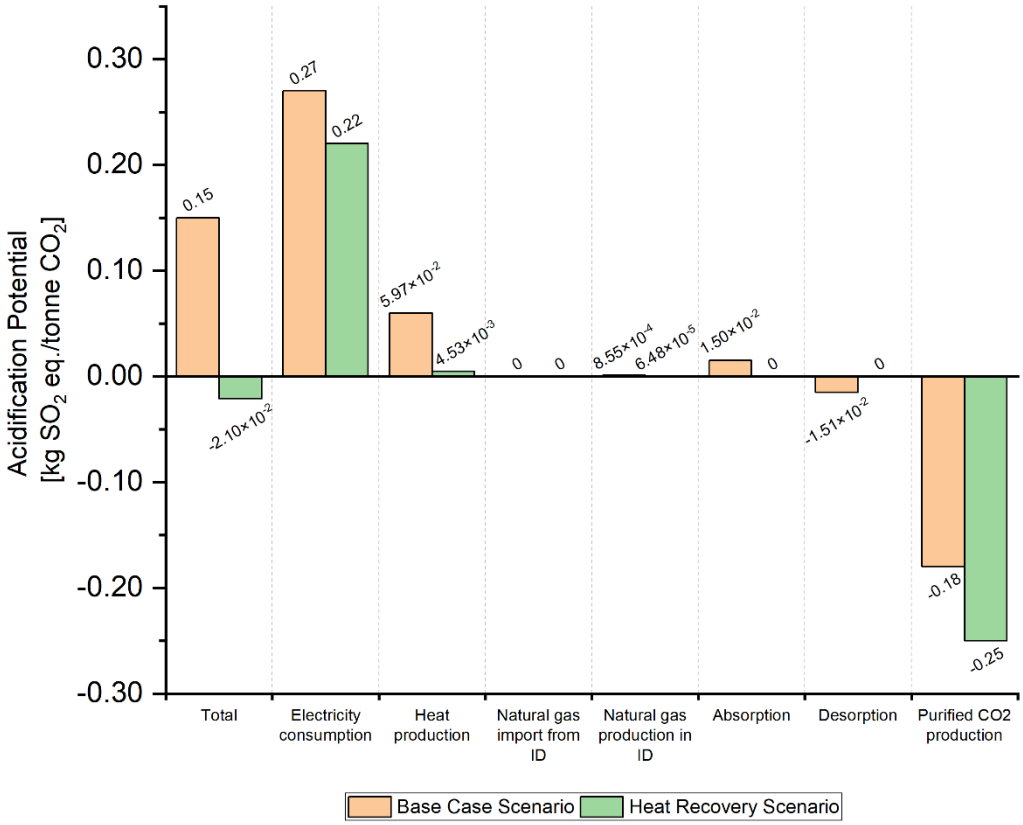

Figure 4. Acidification Potential results for the base case and heat recovery processes, based on an input of one tonne of CO_2.

Eutrophication Potential. The EP results are depicted in Figure 5. Electricity consumption (6.11×10^{-2} kg PO_4 eq.), heat production (1.46×10^{-2} kg PO_4 eq.), and absorption (3.29×10^{-3} kg PO_4 eq.) are the primary elements (95.85%) to Eutrophication Potential (EP) in the base case scenario. For the heat recovery scenario, the main sources are electricity consumption (97.78%), heat production (2.19%), and natural gas production in ID (0.03%). EP is primarily driven by nitrogen oxides, with additional contributions from ammonia and nitrogen. The production of high-purity CO_2 via the base and heat recovery processes reduces EP by 0.36 kg PO_4 eq. and 0.89 kg PO_4 eq., respectively, resulting in an overall reduction of 0.29 kg PO_4 eq. and 0.84 kg PO_4 eq.

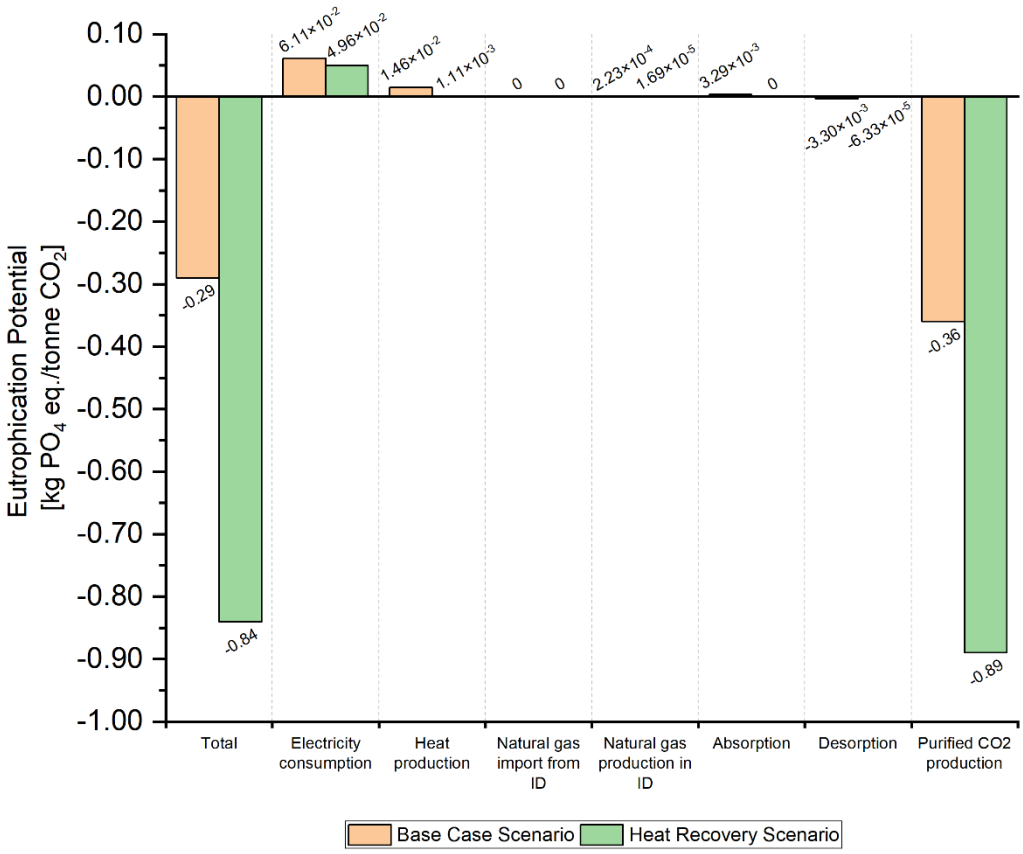

Figure 5. Eutrophication Potential results for the base case and heat recovery processes, based on an input of one tonne of CO_2.

Freshwater Aquatic Ecotoxicity Potential. In both the base case and heat recovery scenarios, the categories ranked from highest to lowest impact on Freshwater Aquatic Ecotoxicity Potential (FAETP) are as follows: heat production (Base Case: 9.08×10^{-3} kg DCB eq.; Heat Recovery: 6.88×10^{-4} kg DCB eq.), electricity consumption (Base Case: 1.42×10^{-4} kg DCB eq.; Heat Recovery: 1.15×10^{-4} kg DCB eq.), natural gas import from ID (Base Case: 4.15×10^{-7} kg DCB eq.; Heat Recovery: 3.15×10^{-8} kg DCB eq.), and natural gas production in ID (Base Case: 7.69×10^{-7} kg DCB eq.; Heat Recovery: 5.83×10^{-8} kg DCB eq.). Heat production makes up 98.45% and 85.64% of FAETP in the base

case and heat recovery scenarios, respectively. Electricity consumption accounts for 1.54% and 14.35% of FAETP in the respective scenarios. The ranking of air pollutants from highest to lowest impact for both scenarios is as follows: formaldehyde (78.95%), mercury (20.96%), benzo(a)pyrene (0.08%), and dioxins (0.01%). The impact of natural gas import and production from ID on FAETP is negligible. Altogether, the base case and heat recovery scenarios contribute a total of 9.22×10^{-3} and 8.04×10^{-4} kg DCB eq. to FAETP, respectively (Figure 6).

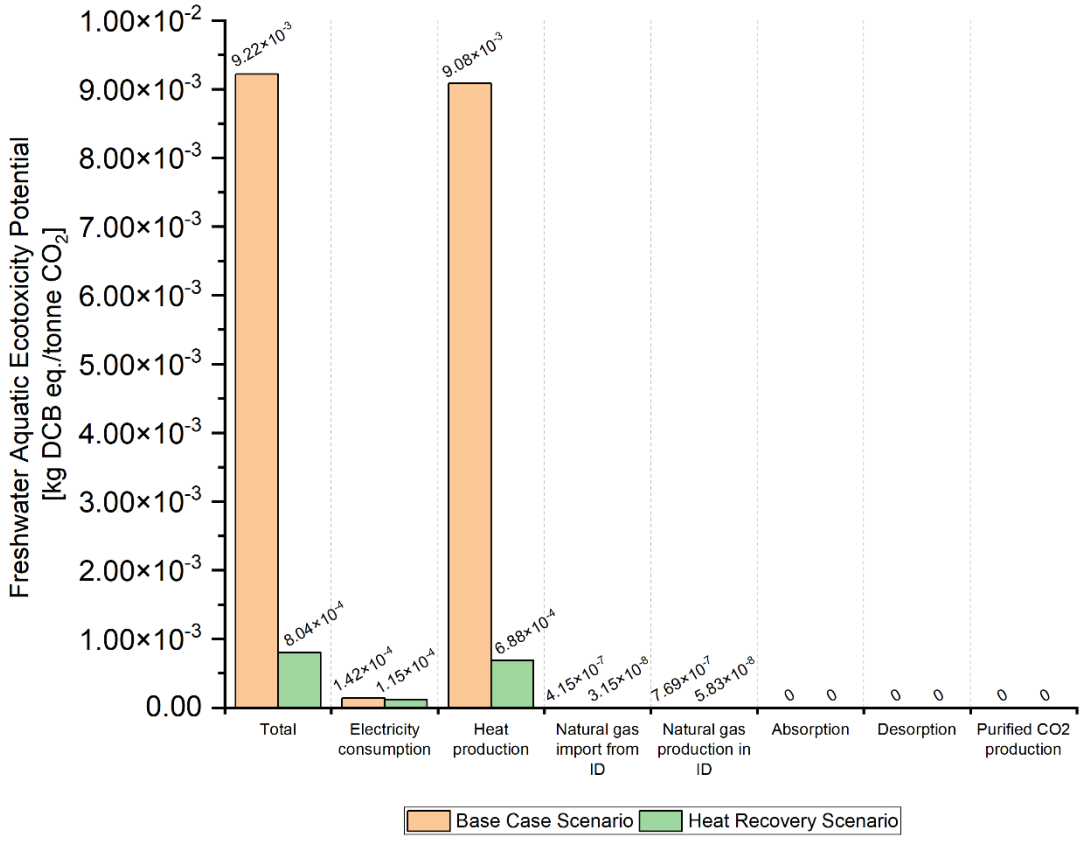

Figure 6. Freshwater Aquatic Ecotoxicity Potential results for the base case and heat recovery processes, based on an input of one tonne of CO_2.

Human Toxicity Potential. In reference to Figure 7, the base case scenario (17.82 kg DCB eq.) exhibits a human toxicity potential (HTP) approximately 10.18 times higher than the heat recovery scenario (1.75 kg DCB eq.). This disparity is primarily due to heat production (Base Case: 17.26 kg DCB eq.; Heat Recovery: 1.31 kg DCB eq.), the most significant factor in HTP. Nitrogen oxides, sulfur dioxide and benzene are the top three substances contributing to HTP in heat production. The next two contributors are electricity consumption (Base Case: 0.57 kg DCB eq.; Heat Recovery: 0.46 kg DCB eq.) and natural gas production in ID (Base Case: 2.03×10^{-3} kg DCB eq.; Heat Recovery: 1.54×10^{-4} kg DCB eq.). The other categories contribute insignificantly to HTP.

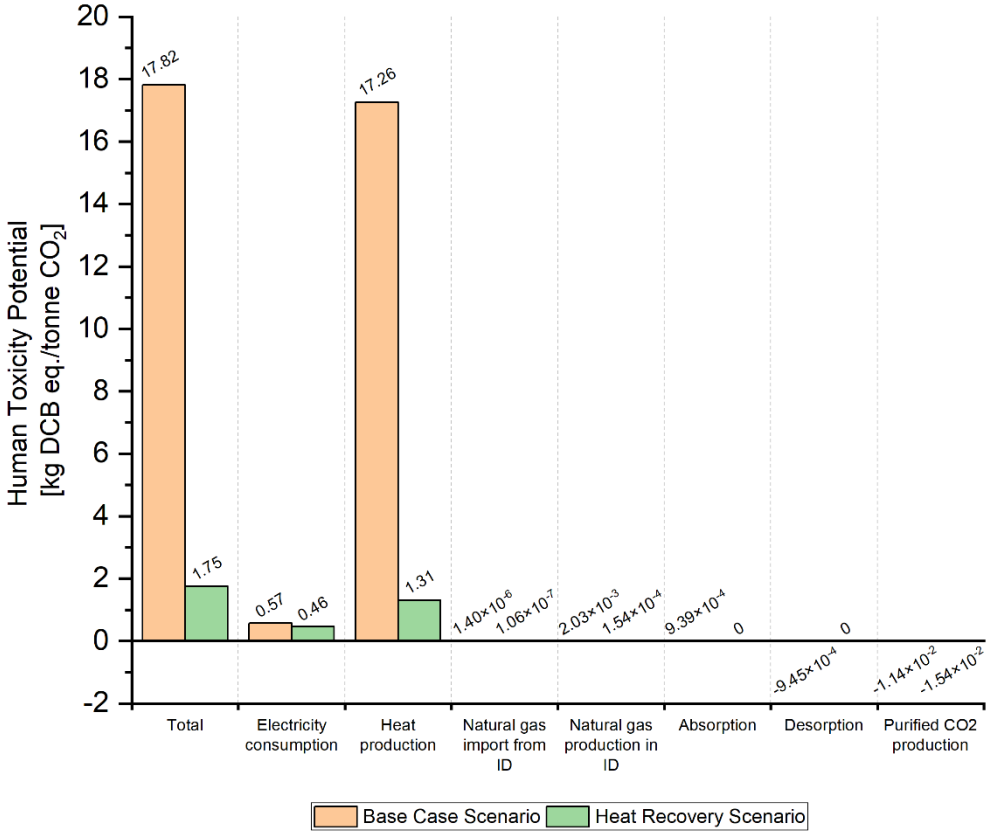

Figure 7. Human Toxicity Potential results for the base case and heat recovery processes, based on an input of one tonne of CO_2.

Marine Aquatic Ecotoxicity Potential. Heat production is the primary driver of Marine Aquatic Ecotoxicity Potential (MAETP), as shown in Figure 8. The heat production process emits mercury, formaldehyde, dioxins, benzo(a)pyrene, benzene, and toluene. In the base case scenario, heat production accounts for 99.78% of MAETP, while in the heat recovery scenario, it accounts for 99.70%. For both scenarios, natural gas production and natural gas import from ID contribute 0.15% and 0.06% of MAETP, respectively. Mercury is emitted during natural gas production in ID and import from ID, while dioxins are released solely from natural gas production in ID. Electricity consumption represents 0.01% of MAETP in the base case and 0.09% in the heat recovery scenario.

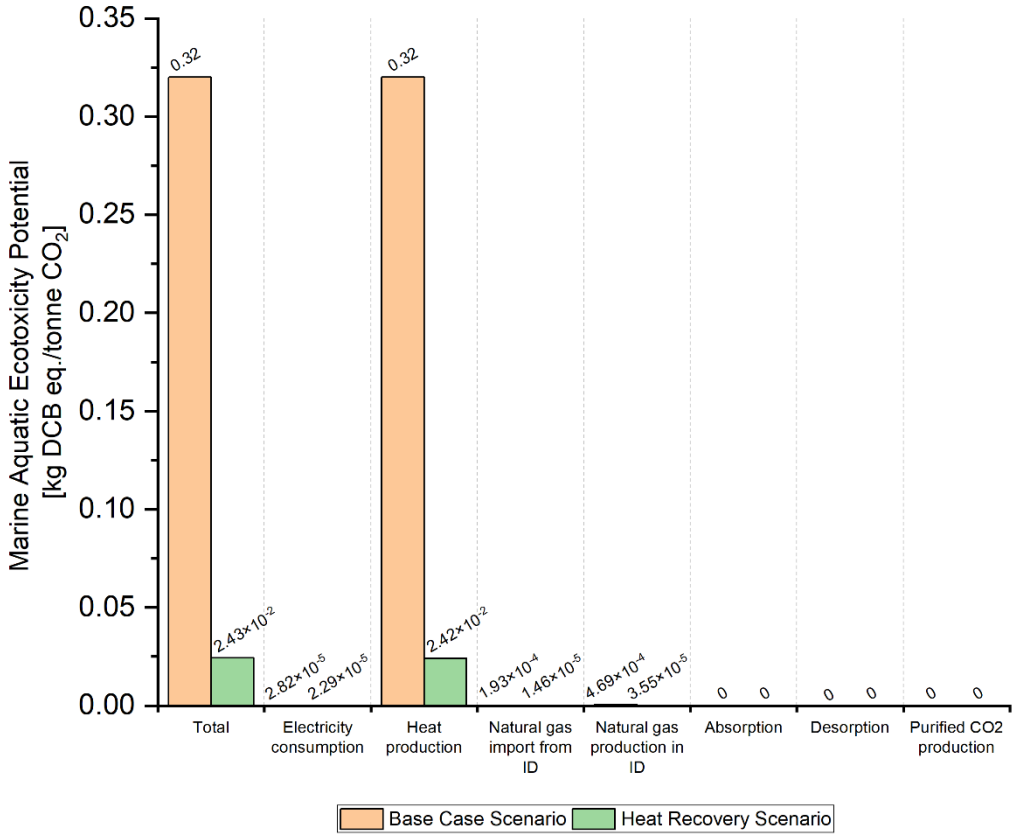

Figure 8. Marine Aquatic Ecotoxicity Potential results for the base case and heat recovery processes, based on an input of one tonne of CO_2.

Photochemical Ozone Creation Potential. Electricity consumption is the most significant contributor to Photochemical Ozone Creation Potential (POCP), accounting for 64.70% in the base case and 95.15% in the heat recovery scenario. This is followed by heat production, which contributes 34.27% in the base case and 4.70% in the heat recovery scenario. Natural gas import from ID accounts for 0.82% in the base case and 0.11% in the heat recovery scenario, while natural gas production in ID contributes 0.22% and 0.03%, respectively. The urban air pollutants contributing to POCP include carbon monoxide, methane, sulfur dioxide, pentane, benzene, toluene, formaldehyde and acetalehyde. The detailed results are illustrated in Figure 9.

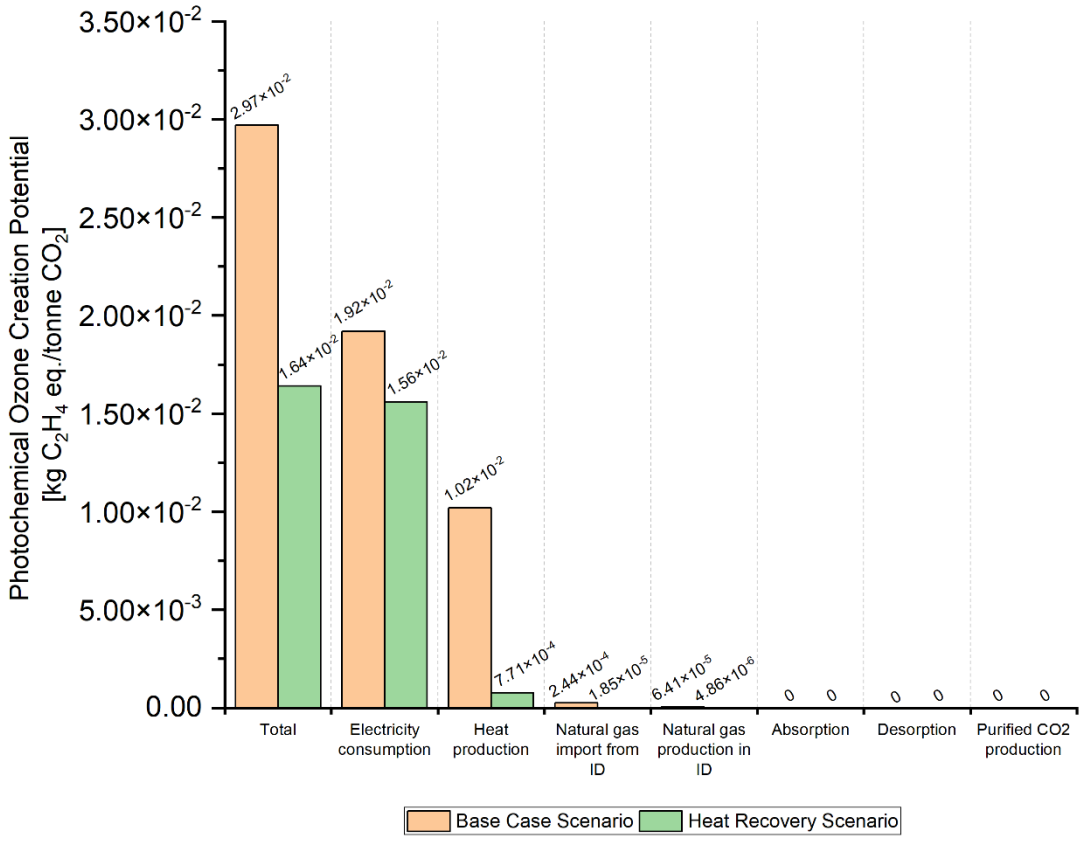

Figure 9. Photochemical Ozone Creation Potential results for the base case and heat recovery processes, based on an input of one tonne of CO_2.

Terrestric Ecotoxicity Potential. Considering Figure 10, heat production is the predominant factor in Terrestrial Ecotoxicity Potential (TETP), representing 99.46% in the base case and 96.89% in the heat recovery scenario. The sources of heat production that add to TETP include benzene, toluene, and formaldehyde. Following this, electricity consumption accounts for 0.27% in the base case and 2.85% in the heat recovery scenario. Natural gas production in ID makes up 0.19% in the base case and 0.18% in the heat recovery scenario, while natural gas import from ID accounts for 0.08% in both scenarios.

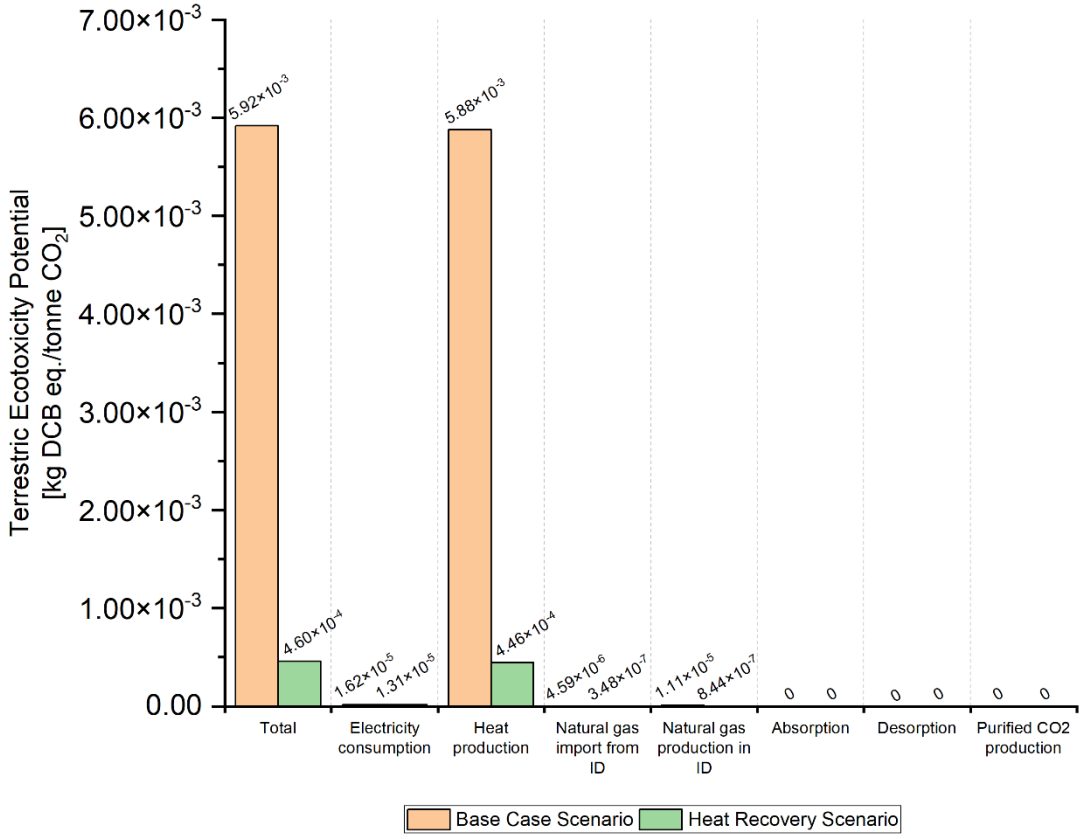

Figure 10. Terrestric Ecotoxicity Potential results for the base case and heat recovery processes, based on an input of one tonne of CO_2.

Overall Environmental Impacts. With the introduction of the heat recovery process, there is a reduction in environmental impacts across all chosen categories. For GWP, the net carbon abatement potential is 94.49 kg CO_2 eq. for the base case scenario and 508.69 kg CO_2 eq. for the heat recovery scenario. The heat recovery scenario can reduce AP by 2.43 $\times 10^{-2}$ kg SO_2 eq., whereas the base case scenario contributes 0.15 kg SO_2 eq. to AP. Both scenarios reduce EP by 0.29 kg PO_4 eq. and 0.84 kg PO_4 eq., respectively. As illustrated in Figure 11, the base case and heat recovery processes also impact FAETP, HTP, MAETP, POCP, and TETP.

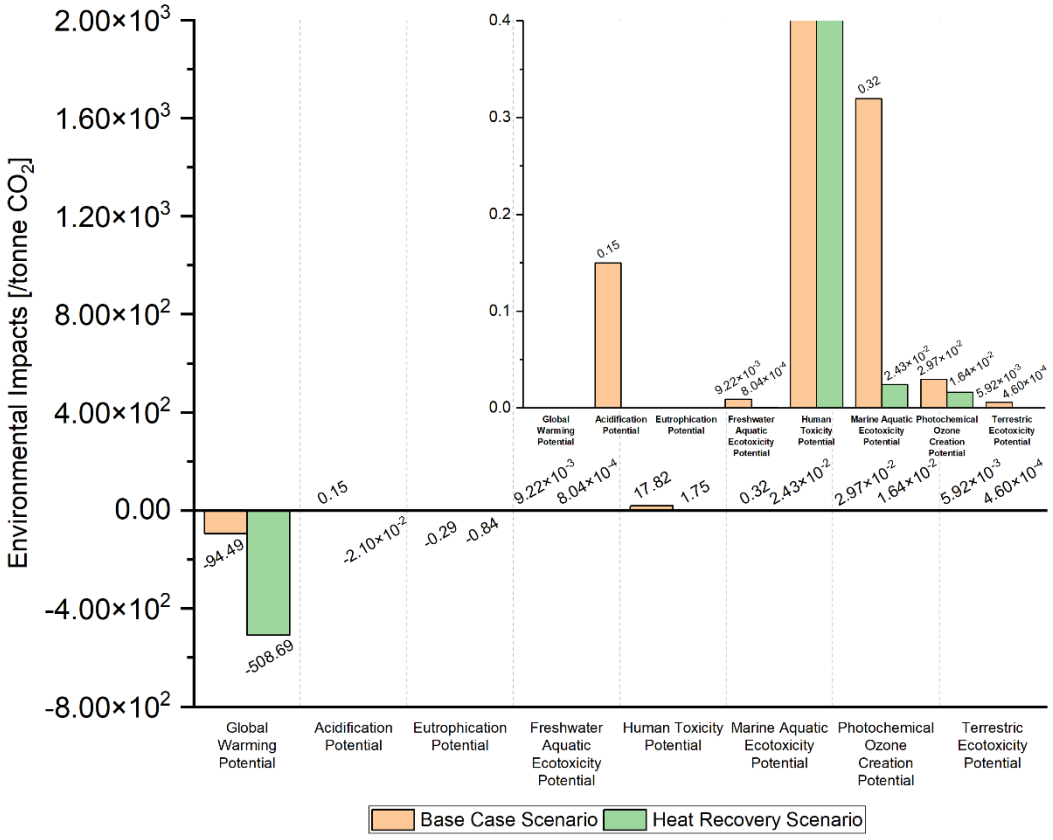

Figure 11. Overall Environmental Impact results for the base case and heat recovery processes, based on an input of one tonne of CO_2.

Sensitivity analysis. Sensitivity analysis in LCA assists in evaluating how the variability of input parameters influences assessment outcomes. For the selected eight environmental impact categories, this analysis involves systematically altering these parameters using the analyst feature of Sphera® LCA for Experts (GaBi) version 10.8.0.14 software[54], applying a standard deviation (SD) of ±20% to the existing electricity and thermal energy consumption of the equipment in the process.[29, 63] In our study, sensitivity analysis helps identify which equipment has the most significant impact, with results expressed in terms of percentage data variation.[64] A higher percentage signifies greater potential variability. Sensitivity analysis enhances the robustness and credibility of our findings by providing an in-depth analysis, clarifying the relationships and interdependencies between various parameters.[65]

Tables 1 to 4 present a comprehensive breakdown of data variation, expressed as a percentage, for each piece of equipment and its total contribution based on electricity and thermal energy consumption for both the base case and heat recovery scenarios. Tables 1 and 3 detail the data variation in electricity consumption, highlighting that the top three environmental impact categories are AP (Base Case: ±16.10%, Heat Recovery: ±19.52%), GWP (Base Case: ±15.77%, Heat Recovery: ±19.52%), and POCP (Base Case: ±12.78%, Heat Recovery: ±19.04%). In the base case scenario, HX01 has the lowest impact, while the auxiliary system has the most significant contribution. This is attributed to the HX01 having the lowest electricity consumption compared to the auxiliary system, which has the highest electricity consumption in our process (Refer to Table S2). The "auxiliary" equipment in this study includes various systems essential for daily plant operations, such as control systems and other necessary machinery. Notably, it primarily comprises the refrigerant unit used for cooling in HX02, HX04, HX05, V01, V02, and V03, which

constitutes a significant portion of the plant's electricity consumption. In the heat recovery scenario, the C02 has the lowest impact, while the auxiliary system again has the highest impact on data variation in electricity consumption.

Table 1. Sensitivity analysis results with ±20% change in electricity consumption of the equipment for the base case simulation model.

Equipment	GWP (%)	AP (%)	EP (%)	FAETP (%)	HTP (%)	POCP (%)	TETP (%)
Flue Gas Cooler (HX01)	±0.03	±0.03	±0.03	NA	NA	±0.03	NA
Compressor (C01)	±0.49	±0.50	±0.50	±0.01	±0.02	±0.40	NA
Pump (P01)	±0.55	±0.57	±0.56	±0.01	±0.02	±0.45	NA
Auxiliary	±14.70	±15.00	±14.70	±0.28	±0.58	±11.90	±0.05
TOTAL	**±15.77**	**±16.10**	**±15.79**	**±0.30**	**±0.62**	**±12.78**	**±0.05**

Table 2. Sensitivity analysis results with ±20% change in thermal energy consumption of the equipment for the base case simulation model.

Equipment	GWP (%)	AP (%)	EP (%)	FAETP (%)	HTP (%)	MAETP (%)	POCP (%)	TETP (%)
Desorber (DSP01)	±4.26	±3.90	±4.17	±19.70	±19.40	±20.00	±7.27	±19.90
TOTAL	**±4.26**	**±3.90**	**±4.17**	**±19.70**	**±19.40**	**±20.00**	**±7.27**	**±19.90**

Table 3. Sensitivity analysis results with ±20% change in electricity consumption of the equipment for the heat recovery simulation model.

Equipment	GWP (%)	AP (%)	EP (%)	FAETP (%)	HTP (%)	MAETP (%)	POCP (%)	TETP (%)
Compressor (C02)	±0.74	±0.74	±0.74	±0.11	±0.20	NA	±0.72	±0.02
Pump (P02)	±2.08	±2.08	±2.08	±0.31	±0.55	NA	±2.02	±0.06
Auxiliary	±16.70	±16.70	±16.70	±2.45	±4.44	±0.02	±16.30	±0.49
TOTAL	**±19.52**	**±19.52**	**±19.52**	**±2.87**	**±5.19**	**±0.02**	**±19.04**	**±0.57**

Table 4. Sensitivity analysis results with ±20% change in thermal energy consumption of the equipment for the heat recovery simulation model.

Equipment	GWP (%)	AP (%)	EP (%)	FAETP (%)	HTP (%)	MAETP (%)	POCP (%)	TETP (%)
Desorber (DSP02)	±0.15	±0.14	±0.15	±5.37	±4.65	±6.27	±0.31	±6.09
Stripper (ST01)	±0.33	±0.30	±0.33	±11.80	±10.20	±13.70	±0.69	±13.30
TOTAL	**±0.48**	**±0.44**	**±0.48**	**±17.17**	**±14.85**	**±19.97**	**±1.00**	**±19.39**

Regarding Tables 2 and 4, the top three environmental impact categories contributing to data variation in thermal energy consumption are MAETP (Base Case: ±20.00%, Heat Recovery: ±19.97%), TETP (Base Case: ±19.90%, Heat Recovery: ±19.39%), and FAETP (Base Case: ±19.70%, Heat Recovery: ±17.17%). ST01 contributes more to data variation across all eight

environmental impact categories compared to DSP02. This may be due to DSP02's lower thermal energy consumption of 4.21×10^7 MJ per operating year compared to ST01's higher thermal energy consumption of 9.22×10^7 MJ per operating year. The difference in energy consumption is likely due to the higher regeneration temperatures required for ST01. The reboiler in ST01 operates at around 100°C, whereas the reboiler in DSP02 operates at approximately 81°C.

In the heat recovery scenario, data variation is higher for electricity consumption compared to the base scenario, whereas data variation for thermal energy consumption is lower. In the base case, it was observed that the energy removed from the system during cooling is indirectly dependent on the heat input to the system. However, with the implementation of heat recovery, this relationship is significantly reduced. The multi-stream heat exchanger facilitates most of the heat removal, thereby reducing the need for supplementary cooling. Supplementary cooling is still required to bring the solvents to the temperatures necessary for the absorption and washing operations.

Additionally, a ±20% change in electricity consumption for the HX01, C01, and P01 in the base case scenario does not result in data variation impacts on TETP (Table 1). Similarly, there is no impact on FAETP and HTP when a ±20% change in electricity consumption is applied to HX01 in the base case. In the heat recovery scenario, a ±20% change in electricity consumption for the C02 and P02 does not lead to data variation impacts on MAETP (Table 3).

Monte Carlo simulation. Monte Carlo simulation is a statistical technique employed in LCA to address the intrinsic uncertainties in results.[66] A spectrum of possible outcomes is generated by repeatedly sampling input data from probability distributions, thereby quantifying uncertainty and variability.[67] Furthermore, the reliability and robustness of the

findings are enhanced by offering a more comprehensive understanding of potential impacts and their probabilities.[68] The application of Monte Carlo simulation improves decision-making by elucidating the range and probability of different outcomes, improving visibility in dealing with uncertainties and recognising key impacting factors.[64]

In our Monte Carlo simulation, we conducted 10,000 iterations applying a standard deviation of 20% for electricity and thermal energy consumption, akin to the settings employed in sensitivity analysis. The outputs are represented as a normal distribution in the Monte Carlo simulation. The results of the Monte Carlo simulation for the base case scenario, with ±20% variations in electricity and thermal energy consumption, are presented in Tables 5 and 6, respectively. For the heat recovery scenarios, corresponding results with ±20% changes in electricity and thermal energy consumption are detailed in Tables 7 and 8, respectively. The median values of GWP, AP, and EP in both the base and heat recovery scenarios (Tables 5 to 8) vary from those in Figure 11, whereas other environmental impact categories demonstrate minimal or no change.

Table 5. Monte Carlo simulation results with ±20% change in electricity consumption of the equipment for the base case simulation model.

Environmental Impact Categories	Median	SD (%)	10% percentile	25% percentile	75% percentile	90% percentile
Global Warming Potential [kg CO_2 eq.]	**4.09**	**160**	**3.3**	**3.68**	**4.49**	**4.84**
Acidification Potential [kg SO_2 eq.]	**3.33×10^{-1}**	**15.0**	**2.68×10^{-1}**	**2.99×10^{-1}**	**3.67×10^{-1}**	**3.97×10^{-1}**
Eutrophication Potential [kg PO_4 eq.]	**7.60×10^{-2}**	**14.70**	**6.14×10^{-2}**	**6.84×10^{-2}**	**8.35×10^{-2}**	**9.02×10^{-2}**
Freshwater Aquatic Ecotoxicity Potential [kg DCB eq.]	**9.22×10^{-3}**	**2.82×10^{-1}**	**9.19×10^{-3}**	**9.21×10^{-3}**	**9.24×10^{-3}**	**9.26×10^{-3}**
Human Toxicity Potential [kg DCB eq.]	**17.80**	**0.58**	**17.70**	**17.80**	**17.90**	**18.00**
Marine Aquatic Ecotoxicity Potential [kg DCB eq.]	**3.20×10^{-1}**	**1.61×10^{-3}**	**3.20×10^{-1}**	**3.20×10^{-1}**	**3.20×10^{-1}**	**3.20×10^{-1}**
Photochemical Ozone Creation Potential [kg C_2H_4 eq.]	**2.97×10^{-2}**	**11.80**	**2.51×10^{-2}**	**2.73×10^{-2}**	**3.21×10^{-2}**	**3.42×10^{-2}**
Terrestric Ecotoxicity Potential [kg DCB eq.]	**5.92×10^{-3}**	**5.00×10^{-2}**	**5.91×10^{-3}**	**5.91×10^{-3}**	**5.92×10^{-3}**	**5.92×10^{-3}**

Table 6. Monte Carlo simulation results with ±20% change in thermal energy consumption of the equipment for the base case simulation model.

Environmental Impact Categories	Median	SD (%)	10% percentile	25% percentile	75% percentile	90% percentile
Global Warming Potential [kg CO_2 eq.]	**4.08**	**176**	**3.86**	**3.96**	**4.20**	**4.30**
Acidification Potential [kg SO_2 eq.]	**3.33×10^{-1}**	**3.89**	**3.16×10^{-1}**	**3.24×10^{-1}**	**3.42×10^{-1}**	**3.50×10^{-1}**
Eutrophication Potential [kg PO_4 eq.]	**7.59×10^{-2}**	**4.16**	**7.19×10^{-2}**	**7.38×10^{-2}**	**7.81×10^{-2}**	**8.00×10^{-2}**
Freshwater Aquatic Ecotoxicity Potential [kg DCB eq.]	**9.23×10^{-3}**	**19.60**	**6.90×10^{-3}**	**8.01×10^{-3}**	**1.05×10^{-2}**	**1.16×10^{-2}**
Human Toxicity Potential [kg DCB eq.]	**17.90**	**19.30**	**13.40**	**15.50**	**20.20**	**22.30**
Marine Aquatic Ecotoxicity Potential [kg DCB eq.]	**3.20×10^{-1}**	**19.90**	**2.38×10^{-1}**	**2.77×10^{-1}**	**3.64×10^{-1}**	**4.02×10^{-1}**
Photochemical Ozone Creation Potential [kg C_2H_4 eq.]	**2.97×10^{-2}**	**7.25**	**2.69×10^{-2}**	**2.82×10^{-2}**	**3.12×10^{-2}**	**3.25×10^{-2}**
Terrestric Ecotoxicity Potential [kg DCB eq.]	**5.92×10^{-3}**	**19.90**	**4.41×10^{-3}**	**5.13×10^{-3}**	**6.73×10^{-3}**	**7.44×10^{-3}**

Table 7. Monte Carlo simulation results with ±20% change in electricity consumption of the equipment for the heat recovery simulation model.

Environmental Impact Categories	Median	SD (%)	10% percentile	25% percentile	75% percentile	90% percentile
Global Warming Potential [kg CO_2 eq.]	**2.72**	**16.90**	**2.13**	**2.41**	**3.02**	**3.31**
Acidification Potential [kg SO_2 eq.]	**2.27×10^{-1}**	**16.90**	**1.77×10^{-1}**	**2.01×10^{-1}**	**2.52×10^{-1}**	**2.75×10^{-1}**
Eutrophication Potential [kg PO_4 eq.]	**5.09×10^{-2}**	**16.90**	**3.98×10^{-2}**	**4.51×10^{-2}**	**5.66×10^{-2}**	**6.19×10^{-2}**
Freshwater Aquatic Ecotoxicity Potential [kg DCB eq.]	**8.04×10^{-4}**	**2.48**	**7.79×10^{-4}**	**7.91×10^{-4}**	**8.17×10^{-4}**	**8.30×10^{-4}**
Human Toxicity Potential [kg DCB eq.]	**1.77**	**4.49**	**1.67**	**1.72**	**1.82**	**1.87**
Marine Aquatic Ecotoxicity Potential [kg DCB eq.]	**2.43×10^{-2}**	**1.63×10^{-2}**	**2.42×10^{-2}**	**2.43×10^{-2}**	**2.43×10^{-2}**	**2.43×10^{-2}**
Photochemical Ozone Creation Potential [kg C_2H_4 eq.]	**1.64×10^{-2}**	**16.40**	**1.30×10^{-2}**	**1.46×10^{-2}**	**1.82×10^{-2}**	**1.98×10^{-2}**
Terrestric Ecotoxicity Potential [kg DCB eq.]	**4.61×10^{-4}**	**4.94×10^{-1}**	**4.58×10^{-4}**	**4.59×10^{-4}**	**4.62×10^{-4}**	**4.63×10^{-4}**

Table 8. Monte Carlo simulation results with ±20% change in thermal energy consumption of the equipment for the heat recovery simulation model.

Environmental Impact Categories	Median	SD (%)	10% percentile	25% percentile	75% percentile	90% percentile
Global Warming Potential [kg CO_2 eq.]	**2.71**	**3.63×10^{-1}**	**2.70**	**2.71**	**2.72**	**2.73**
Acidification Potential [kg SO_2 eq.]	**2.26×10^{-1}**	**3.26×10^{-1}**	**2.25×10^{-1}**	**2.25×10^{-1}**	**2.26×10^{-1}**	**2.27×10^{-1}**
Eutrophication Potential [kg PO_4 eq.]	**5.07×10^{-2}**	**3.53×10^{-1}**	**5.05×10^{-2}**	**5.06×10^{-2}**	**5.08×10^{-2}**	**5.10×10^{-2}**
Freshwater Aquatic Ecotoxicity Potential [kg DCB eq.]	**8.04×10^{-4}**	**12.80**	**6.72×10^{-4}**	**7.34×10^{-4}**	**8.74×10^{-4}**	**9.36×10^{-4}**
Human Toxicity Potential [kg DCB eq.]	**1.77**	**11.10**	**1.52**	**1.64**	**1.90**	**2.02**
Marine Aquatic Ecotoxicity Potential [kg DCB eq.]	**2.43×10^{-2}**	**14.90**	**1.96×10^{-2}**	**2.18×10^{-2}**	**2.67×10^{-2}**	**2.89×10^{-2}**
Photochemical Ozone Creation Potential [kg C_2H_4 eq.]	**1.64×10^{-2}**	**7.45×10^{-1}**	**1.62×10^{-2}**	**1.63×10^{-2}**	**1.65×10^{-2}**	**1.66×10^{-2}**
Terrestric Ecotoxicity Potential [kg DCB eq.]	**4.61×10^{-4}**	**14.50**	**3.75×10^{-4}**	**4.15×10^{-4}**	**5.06×10^{-4}**	**5.46×10^{-4}**

When comparing the base case with the heat recovery scenario, where there was a ±20% change in electricity consumption, all impacts across the eight categories were reduced in the heat recovery scenario. The implementation of a heat exchanger in the heat recovery scenario indirectly results in electricity consumption savings. However, the standard deviation (SD) for seven categories in Table 7 increased in the heat recovery scenario compared to Table 5, except for GWP, where the SD decreased by a factor of 9.47.

When comparing the base case with the heat recovery scenario, where there was a ±20% change in thermal energy consumption, all impacts across the eight categories diminished in the heat recovery scenario. The multi-stream heat exchanger significantly minimizes the need for external heat inputs by efficiently utilizing internal heat streams. Additionally, the SD across all eight environmental impact categories in Table 8 (heat recovery scenario) declined compared to Table 6 (base case scenario). The SD for GWP exhibited the most notable decrease, dropping from 176 to 3.63×10^{-1}, representing a reduction by a factor of 484.85. Lower standard deviation improves consistency and reduces variability in outcomes. It enhances the reliability of decision-making by providing greater certainty in the expected range of estimated impacts under study.

Scenario analysis. Scenario analysis in LCA entails assessing the environmental performance of a product, process, or system under different conditions or assumptions.[69] This approach enhances understanding, supports informed decision-making, and enables the comparison of alternative scenarios. By analyzing variations in key parameters, it helps identify strategies for improving sustainability.[69] In this scenario analysis, we examine three distinct parameters. The first and second scenarios involve modifying the electricity profile from SG to those of the U.S. and EU, respectively, for both the base case and the heat recovery scenario. In the third scenario, an acid wash is added to the heat recovery model to reduce ammonia emissions.[29]

The electricity production datasets for the U.S. and EU are obtained from Ecoinvent v3.9.1.[56] The U.S. dataset represents high-voltage electricity generation in a natural gas combined cycle power plant, while the European dataset corresponds to electricity production using compressed air energy storage. Further details on these datasets are provided in Table S5 of the SI. The overall environmental impact results for the base case (SG, U.S., EU), heat recovery (SG, U.S., EU), and heat recovery with acid wash scenarios, based on an input of one tonne of CO_2, are summarized in Table 9.

Table 9. Overall environmental impact results for the base case (SG, U.S., EU), heat recovery (SG, U.S., EU), and heat recovery with acid wash scenarios, based on an input of one tonne of CO_2.

Environmental Impact Categories	Base Case (SG)	Base Case (U.S.)	Base Case (EU)	Heat Recovery (SG)	Heat Recovery (U.S.)	Heat Recovery (EU)	Heat Recovery with Acid Wash (SG)
Global Warming Potential [kg CO_2 eq.]	**-94.49**	**-223.87**	**-352.84**	**-508.69**	**-613.80**	**-718.57**	**-462.09**
Acidification Potential [kg SO_2 eq.]	**1.50×10^{-1}**	**-1.46×10^{-2}**	**-9.78×10^{-2}**	**-2.10×10^{-2}**	**-1.55×10^{-1}**	**-2.22×10^{-1}**	**8.23**
Eutrophication Potential [kg PO_4 eq.]	**-2.86×10^{-1}**	**-3.10×10^{-1}**	**-3.41×10^{-1}**	**-8.37×10^{-1}**	**-8.56×10^{-1}**	**-8.81×10^{-1}**	**-8.29×10^{-1}**
Freshwater Aquatic Ecotoxicity Potential [kg DCB eq.]	**9.22×10^{-3}**	**9.49**	**1.12×10^{-2}**	**8.04×10^{-4}**	**7.70**	**2.44×10^{-3}**	**4.58×10^{-1}**
Human Toxicity Potential [kg DCB eq.]	**17.82**	**35.58**	**20.33**	**1.75**	**16.18**	**3.79**	**10.55**
Marine Aquatic Ecotoxicity Potential [kg DCB eq.]	**3.20×10^{-1}**	**1.51×10^{4}**	**6.38**	**2.43×10^{-2}**	**1.22×10^{4}**	**4.95**	**4.61×10^{3}**
Photochemical Ozone Creation Potential [kg C_2H_4 eq.]	**2.97×10^{-2}**	**7.86×10^{-2}**	**1.46×10^{-2}**	**1.64×10^{-2}**	**5.61×10^{-2}**	**4.18×10^{-3}**	**3.42×10^{-1}**
Terrestric Ecotoxicity	**5.92×10^{-3}**	**4.01×10^{-1}**	**1.13×10^{-2}**	**4.60×10^{-4}**	**3.22×10^{-1}**	**4.87×10^{-3}**	**1.75×10^{-1}**

Potential
[kg DCB eq.]

When comparing the base case and heat recovery scenarios for the electricity profiles of SG, U.S., and EU, the European scenarios (both Base Case and Heat Recovery) demonstrate the best performance in multiple environmental impact categories, including GWP, AP, EP, and POCP. For GWP, the values are -352.84 kg CO_2 eq. for the Base Case (EU) and -718.57 kg CO_2 eq. for Heat Recovery (EU). The European scenarios achieve greater overall CO_2 abatement due to the lower emissions associated with their electricity generation. In AP, the Base Case (EU) yields -9.78×10^{-2} kg SO_2 eq., while Heat Recovery (EU) gives -2.22×10^{-1} kg SO_2 eq. This is due to the lower emissions of nitrogen oxides and sulfur dioxide compared to the SG and U.S. scenarios. For EP, the results are -3.41×10^{-1} kg PO_4 eq. for the Base Case (EU) and -8.81×10^{-1} kg PO_4 eq. for Heat Recovery (EU). Nitrogen oxides are the primary contributor to EP, and the European scenarios exhibit the lowest impact from these emissions. For POCP, the values are 1.46×10^{-2} kg C_2H_4 eq. for the Base Case (EU) and 4.18×10^{-3} kg C_2H_4 eq. for Heat Recovery (EU). The European scenarios showed the lowest POCP impact due to pollutants such as carbon monoxide, methane and sulphur dioxide.

Conversely, SG's scenarios (Base Case and Heat Recovery) exhibit the lowest environmental impacts across other categories. For FAETP, the Base Case (SG) registers 9.22×10^{-3} kg DCB eq., while Heat Recovery (SG) records 8.04×10^{-4} kg DCB eq. HTP shows 17.82 kg DCB eq. for the Base Case (SG) and 1.75 kg DCB eq. for Heat Recovery (SG). MAETP values are 3.20×10^{-1} kg DCB eq. for the Base Case (SG) and 2.43×10^{-2} kg DCB eq. for Heat Recovery (SG). Finally, TETP yields 5.92×10^{-3} kg DCB eq. in the Base Case (SG) and 4.60×10^{-4} kg DCB eq. in Heat Recovery (SG). This is because SG's

electricity generation contributes less to pollutant emissions affecting FAETP, HTP, MAETP, and TETP compared to the datasets used for U.S. and EU electricity generation.

In comparing the Heat Recovery (SG) scenario to the Heat Recovery with Acid Wash (SG) scenario, the former exhibited lower environmental impacts across all categories. This is due to the sulfur process, which contributed to all environmental impact categories, while the sulfuric acid process specifically influenced AP and HTP in the Heat Recovery with Acid Wash (SG) scenario.

CONCLUSION

In this study, we introduced a base case and a heat recovery scenario focused on capturing and utilizing low-concentration CO_2 from the flue gas of NGCC power plants using aqueous ammonia. Detailed descriptions of these processes are provided in the Materials and Methods section, with both designed to capture 300 kilotonnes of CO_2 per operating year. Cradle-to-gate LCA was performed and compared for both industrial-scale processes, using a functional unit of per tonne CO_2 input.

The results revealed a net carbon abatement of 94.49 kg CO_2 eq. for the base case and 508.69 kg CO_2 eq. for the heat recovery scenario. Electricity consumption and heat production were identified as the major contributors to GWP. The Impact Assessment results identified HTP and MAETP as the primary environmental impact categories to target for reducing overall impacts. Heat production was the major contributor to HTP, followed by electricity consumption. The top three air contaminants contributing to HTP in heat production were nitrogen oxides, sulfur dioxide, and benzene. For MAETP, heat production was the primary factor, accounting for as much as 99.78% in the base case scenario. Air pollutants released during heat production included mercury, formaldehyde, dioxins, benzo(a)pyrene, benzene, and toluene. Overall, the implementation of the heat recovery process has led to a reduction in environmental impacts across all eight studied categories.

Sensitivity analysis and Monte Carlo simulation were performed by applying a standard deviation of ±20% to the existing electricity and thermal energy consumption of the equipment. This approach identifies key parameters that significantly influence outcomes and helps understand uncertainties and confidence in the results. The auxiliary system exhibited the largest

data variation across all the investigated environmental impact categories in both the base case and heat recovery simulation models. In the heat recovery simulation model, ST01 showed greater data variation for a ±20% change in thermal energy consumption compared to DSP02. The Monte Carlo simulation indicated changes in the median values of GWP, AP, and EP in both scenarios, while other environmental impact categories showed minimal or no change in median values.

The conducted scenario analysis involved the adaptation of electricity profiles from SG to those of the U.S. and the EU for both the base case and heat recovery processes. Additionally, an acid wash was integrated into the heat recovery process to decrease ammonia emissions. The findings indicate that the European scenarios, encompassing both the Base Case and Heat Recovery, exhibited the most favorable outcomes across various environmental impact categories, such as GWP, AP, EP, and POCP. In contrast, the scenarios for Singapore yielded the lowest environmental impacts in several other categories. This trend can be attributed to Singapore's electricity generation, which is associated with reduced pollutant emissions that influence FAETP, HTP, MAETP, and TETP compared to the datasets for the U.S. and EU. Furthermore, a comparison of the Heat Recovery (SG) scenario and the Heat Recovery with Acid Wash (SG) scenario revealed that the former consistently exhibited lower environmental impacts across all assessed categories.

Carbon capture technology, as described in this work, provides a solution for sustainable power generation and helps other industries minimize their emissions. While the heat recovery process has successfully reduced environmental impacts relative to the base case scenario, opportunities for further enhancement remain. Implementing more energy-efficient equipment and higher-efficiency heat exchangers could further decrease electricity

and thermal energy needs. We are also investigating ways to refine our process to achieve even higher purity CO_2.

To enhance our LCA efforts, we plan to investigate our technology at a pilot plant scale, which will provide a more accurate representation of the processes, particularly regarding supply chain activities within the system boundary. Future studies will focus on optimizing the integration of ammonia-based CO_2 capture with industrial waste carbonation. In addition, we aim to simulate larger-scale scenarios that exceed the annual capture of 300 kilotonnes of CO_2. By comparing our LCA results with those from various CCS technologies, we seek to identify the most viable options. Furthermore, we will conduct techno-economic assessments to evaluate the cost-effectiveness of our processes, ensuring a comprehensive understanding of their potential impact and feasibility.

ASSOCIATED CONTENT

Supporting Information.

The following file is available free of charge at "insert link".

Information on life cycle inventories for the base case and heat recovery simulation models, snapshots of the base case and heat recovery simulation LCA models (PDF).

AUTHOR INFORMATION

Corresponding Authors

Pancy Ang – *Institute of Sustainability for Chemicals, Energy and Environment, Jurong Island, Singapore;* Phone: +65-6796-3733; Email: pancy_ang@isce2.a-star.edu.sg

Cheng Shuying – *Institute of Sustainability for Chemicals, Energy and Environment, Jurong Island, Singapore;* Phone: +65-6796-3945; Email: cheng_shuying@isce2.a-star.edu.sg

ACKNOWLEDGMENT

We gratefully acknowledge the Agency for Science, Technology and Research (A*STAR), Science and Engineering Research Council (SERC) for funding this research under the Low-Carbon Energy Research Funding Initiative (Project Ref.: U2102d2008). This research is supported by the National Research Foundation, Singapore.

REFERENCES

1. Lüthi, D.; Le Floch, M.; Bereiter, B.; Blunier, T.; Barnola, J.-M.; Siegenthaler, U.; Raynaud, D.; Jouzel, J.; Fischer, H.; Kawamura, K.; Stocker, T. F., High-resolution carbon dioxide concentration record 650,000–800,000 years before present. *Nature* **2008,** *453* (7193), 379-382, DOI 10.1038/nature06949.
2. Agency, I. E. How much CO2 do countries in Europe emit? https://www.iea.org/regions/europe/emissions#how-much-co2-do-countries-in-europe-emit (accessed 26 July 2024).
3. Agency, I. E. How much CO2 does China emit? https://www.iea.org/countries/china/emissions#how-much-co2-does-china-emit (accessed 26 July 2024).
4. Agency, I. E. How much CO2 do countries in Asia Pacific emit? https://www.iea.org/regions/asia-pacific/emissions#how-much-co2-do-countries-in-asia-pacific-emit (accessed 26 July 2024).
5. Paltsev, S.; Morris, J.; Kheshgi, H.; Herzog, H., Hard-to-Abate Sectors: The role of industrial carbon capture and storage (CCS) in emission mitigation. *Applied Energy* **2021,** *300*, 117322, DOI 10.1016/j.apenergy.2021.117322.
6. Tan, Y.; Nookuea, W.; Li, H.; Thorin, E.; Yan, J., Property impacts on Carbon Capture and Storage (CCS) processes: A review. *Energy Conversion and Management* **2016,** *118*, 204-222, DOI 10.1016/j.enconman.2016.03.079.
7. Dziejarski, B.; Krzyżyńska, R.; Andersson, K., Current status of carbon capture, utilization, and storage technologies in the global economy: A survey of technical assessment. *Fuel* **2023,** *342*, 127776, DOI 10.1016/j.fuel.2023.127776.
8. Hasan, M. M. F.; First, E. L.; Boukouvala, F.; Floudas, C. A., A multi-scale framework for CO2 capture, utilization, and sequestration: CCUS and CCU. *Computers & Chemical Engineering* **2015,** *81*, 2-21, DOI 10.1016/j.compchemeng.2015.04.034.
9. Agency, U. S. E. P. Greenhouse Gas Emissions in the Electric Power Sector by Fuel Source. https://www.epa.gov/ghgemissions/sources-greenhouse-gas-emissions (accessed 26 July 2024).
10. Secretariat, N. C. C. OVERVIEW. https://www.nccs.gov.sg/singapores-climate-action/overview/national-circumstances/ (accessed 26 July 2024).
11. Badr Al Hashmi, A., Aziz Abdulla Mohamed, A. and Eddine Dadach, Z., Process Simulation of a 620 Mw-Natural Gas Combined Cycle Power Plant with Optimum Flue Gas Recirculation. *Open Journal of Energy Efficiency* **2018,** *7*, 33-52, DOI 10.4236/ojee.2018.72003.
12. Hu, Y.; Gao, Y.; Lv, H.; Xu, G.; Dong, S., A New Integration System for Natural Gas Combined Cycle Power Plants with CO2 Capture and Heat Supply. **2018,** *11* (11), 3055, DOI 10.3390/en11113055.
13. Davison, J., Performance and costs of power plants with capture and storage of CO2. *Energy* **2007,** *32* (7), 1163-1176, DOI 10.1016/j.energy.2006.07.039.
14. MacDowell, N.; Florin, N.; Buchard, A.; Hallett, J.; Galindo, A.; Jackson, G.; Adjiman, C. S.; Williams, C. K.; Shah, N.; Fennell, P., An overview of CO2 capture technologies. *Energy & Environmental Science* **2010,** *3* (11), 1645-1669, DOI 10.1039/C004106H.
15. Li, S.; Xu, Y.; Gao, Q., Measurements and modelling of oxy-fuel coal combustion. *Proceedings of the Combustion Institute* **2019,** *37* (3), 2643-2661, DOI 10.1016/j.proci.2018.08.054.
16. Stanger, R.; Wall, T.; Spörl, R.; Paneru, M.; Grathwohl, S.; Weidmann, M.; Scheffknecht, G.; McDonald, D.; Myöhänen, K.; Ritvanen, J.; Rahiala, S.; Hyppänen, T.; Mletzko, J.; Kather, A.; Santos, S., Oxyfuel combustion for CO2 capture in power plants. *International Journal of Greenhouse Gas Control* **2015,** *40*, 55-125, DOI 10.1016/j.ijggc.2015.06.010.
17. Yin, C.; Yan, J., Oxy-fuel combustion of pulverized fuels: Combustion fundamentals and modeling. *Applied Energy* **2016,** *162*, 742-762, DOI 10.1016/j.apenergy.2015.10.149.
18. Hu, Y.; Xu, G.; Xu, C.; Yang, Y., Thermodynamic analysis and techno-economic evaluation of an integrated natural gas combined cycle (NGCC) power plant with post-combustion CO2 capture. *Applied Thermal Engineering* **2017,** *111*, 308-316, DOI 10.1016/j.applthermaleng.2016.09.094.
19. Lepaumier, H.; Picq, D.; Carrette, P. L., Degradation study of new solvents for CO2 capture in post-combustion. *Energy Procedia* **2009,** *1* (1), 893-900, DOI 10.1016/j.egypro.2009.01.119.
20. Chowdhury, F. A.; Goto, K.; Yamada, H.; Matsuzaki, Y., A screening study of alcohol solvents for alkanolamine-based CO2 capture. *International Journal of Greenhouse Gas Control* **2020,** *99*, 103081, DOI 10.1016/j.ijggc.2020.103081.
21. Choubtashani, S.; Rashidi, H., CO2 capture process intensification of water-lean methyl diethanolamine-piperazine solvent: Experiments and response surface modeling. *Energy* **2023,** *267*, 126447, DOI 10.1016/j.energy.2022.126447.

22. Lawal, O.; Bello, A.; Idem, R., The Role of Methyl Diethanolamine (MDEA) in Preventing the Oxidative Degradation of CO2 Loaded and Concentrated Aqueous Monoethanolamine (MEA)−MDEA Blends during CO2 Absorption from Flue Gases. *Industrial & Engineering Chemistry Research* **2005,** *44* (6), 1874-1896, DOI 10.1021/ie049261y.
23. Islam, M. S.; Dhanavath, K. N.; Kao, N.; Bhattacharjee, P. K.; Ali, B. S.; RozitaYusoff, Carbon dioxide induced degradation of diethanolamine during absorption and desorption processes. *Chinese Journal of Chemical Engineering* **2018,** *26* (2), 293-302, DOI 10.1016/j.cjche.2017.06.003.
24. Zhang, Y.; Freeman, B.; Hao, P.; Rochelle, G. T., Absorber modeling for NGCC carbon capture with aqueous piperazine. *Faraday Discussions* **2016,** *192* (0), 459-477, DOI 10.1039/C6FD00030D.
25. Rochelle, G. T., Amine Scrubbing for CO2 Capture. **2009,** *325* (5948), 1652-1654, DOI 10.1126/science.1176731.
26. Luo, X.; Wang, M.; Chen, J., Heat integration of natural gas combined cycle power plant integrated with post-combustion CO2 capture and compression. *Fuel* **2015,** *151*, 110-117, DOI 10.1016/j.fuel.2015.01.030.
27. Han, K.; Ahn, C. K.; Lee, M. S.; Rhee, C. H.; Kim, J. Y.; Chun, H. D., Current status and challenges of the ammonia-based CO2 capture technologies toward commercialization. *International Journal of Greenhouse Gas Control* **2013,** *14*, 270-281, DOI 10.1016/j.ijggc.2013.01.007.
28. Jilvero, H.; Mathisen, A.; Eldrup, N.-H.; Normann, F.; Johnsson, F.; Müller, G. I.; Melaaen, M. C., Techno-economic Analysis of Carbon Capture at an Aluminum Production Plant – Comparison of Post-combustion Capture Using MEA and Ammonia. *Energy Procedia* **2014,** *63*, 6590-6601, DOI 10.1016/j.egypro.2014.11.695.
29. Ang, P.; Goh, W.; Bu, J.; Cheng, S., Assessing Carbon Capture and Carbonation in Recycled Concrete Aggregates: A Holistic Life Cycle Assessment Perspective with Simulation at Industrial Scale. *Journal of Cleaner Production* **2024,** *474*, 143553, DOI 10.1016/j.jclepro.2024.143553.
30. Yu, H.; Qi, G.; Xiang, Q.; Wang, S.; Fang, M.; Yang, Q.; Wardhaugh, L.; Feron, P., Aqueous Ammonia Based Post Combustion Capture: Results from Pilot Plant Operation, Challenges and Further Opportunities. *Energy Procedia* **2013,** *37*, 6256-6264, DOI 10.1016/j.egypro.2013.06.554.
31. Wang, F.; Zhao, J.; Miao, H.; Zhao, J.; Zhang, H.; Yuan, J.; Yan, J., Current status and challenges of the ammonia escape inhibition technologies in ammonia-based CO2 capture process. *Applied Energy* **2018,** *230*, 734-749, DOI 10.1016/j.apenergy.2018.08.116.
32. Gaspar, J.; Arshad, M. W.; Blaker, E. A.; Langseth, B.; Hansen, T.; Thomsen, K.; von Solms, N.; Fosbøl, P. L., A Low Energy Aqueous Ammonia CO2 Capture Process. *Energy Procedia* **2014,** *63*, 614-623, DOI 10.1016/j.egypro.2014.11.066.
33. Pinsent, B. R. W.; Pearson, L.; Roughton, F. J. W., The kinetics of combination of carbon dioxide with ammonia. *Transactions of the Faraday Society* **1956,** *52* (0), 1594-1598, DOI 10.1039/TF9565201594.
34. Diao, Y.-F.; Zheng, X.-Y.; He, B.-S.; Chen, C.-H.; Xu, X.-C., Experimental study on capturing CO2 greenhouse gas by ammonia scrubbing. *Energy Conversion and Management* **2004,** *45* (13), 2283-2296, DOI 10.1016/j.enconman.2003.10.011.
35. Zhao, B.; Su, Y.; Tao, W.; Li, L.; Peng, Y., Post-combustion CO2 capture by aqueous ammonia: A state-of-the-art review. *International Journal of Greenhouse Gas Control* **2012,** *9*, 355-371, DOI 10.1016/j.ijggc.2012.05.006.
36. Eigbe, P. A.; Ajayi, O. O.; Olakoyejo, O. T.; Fadipe, O. L.; Efe, S.; Adelaja, A. O., A general review of CO2 sequestration in underground geological formations and assessment of depleted hydrocarbon reservoirs in the Niger Delta. *Applied Energy* **2023,** *350*, 121723, DOI 10.1016/j.apenergy.2023.121723.
37. Norhasyima, R. S.; Mahlia, T. M. I., Advances in CO_2 utilization technology: A patent landscape review. *Journal of CO2 Utilization* **2018,** *26*, 323-335, DOI 10.1016/j.jcou.2018.05.022.
38. Ramdon Applications of Beverage Grade CO2: Industry Uses and Benefits. https://ramdon.com/applications-of-beverage-grade-co2/ (accessed 26 July 2024).
39. Online, D. Carbon dioxide. https://go.drugbank.com/drugs/DB09157 (accessed 26 July 2024).
40. Ghiat, I.; Al-Ansari, T., A review of carbon capture and utilisation as a CO2 abatement opportunity within the EWF nexus. *Journal of CO2 Utilization* **2021,** *45*, 101432, DOI 10.1016/j.jcou.2020.101432.
41. Chauvy, R.; Meunier, N.; Thomas, D.; De Weireld, G., Selecting emerging CO2 utilization products for short- to mid-term deployment. *Applied Energy* **2019,** *236*, 662-680, DOI 10.1016/j.apenergy.2018.11.096.
42. Nimmas, T.; Wongsakulphasatch, S.; Chanthanumataporn, M.; Vacharanukrauh, T.; Assabumrungrat, S., Thermochemical transformation of CO2 into high-value products. *Current Opinion in Green and Sustainable Chemistry* **2024,** *47*, 100911, DOI 10.1016/j.cogsc.2024.100911.

43. Kamkeng, A. D. N.; Wang, M.; Hu, J.; Du, W.; Qian, F., Transformation technologies for CO2 utilisation: Current status, challenges and future prospects. *Chemical Engineering Journal* **2021,** *409*, 128138, DOI 10.1016/j.cej.2020.128138.
44. Strube, R.; Pellegrini, G.; Manfrida, G., The environmental impact of post-combustion CO2 capture with MEA, with aqueous ammonia, and with an aqueous ammonia-ethanol mixture for a coal-fired power plant. *Energy* **2011,** *36* (6), 3763-3770, DOI 10.1016/j.energy.2010.12.060.
45. Štefanica, J.; Smutná, J.; Kočí, V.; Machač, P.; Pilař, L., Environmental Gains and Impacts of a CCS Technology – Case Study of Post-combustion CO2 Separation by Ammonia Absorption. *Energy Procedia* **2016,** *86*, 215-218, DOI 10.1016/j.egypro.2016.01.022.
46. Petrescu, L.; Bonalumi, D.; Valenti, G.; Cormos, A.-M.; Cormos, C.-C., Life Cycle Assessment for supercritical pulverized coal power plants with post-combustion carbon capture and storage. *Journal of Cleaner Production* **2017,** *157*, 10-21, DOI 10.1016/j.jclepro.2017.03.225.
47. Matin, N. S.; Flanagan, W. P., Life cycle assessment of amine-based versus ammonia-based post combustion CO2 capture in coal-fired power plants. *International Journal of Greenhouse Gas Control* **2022,** *113*, 103535, DOI 10.1016/j.ijggc.2021.103535.
48. Schmitt, T.; Leptinsky, S.; Turner, M.; Zoelle, A.; White, C. W.; Hughes, S.; Homsy, S.; Woods, M.; Hoffman, H.; Shultz, T.; James III, R. E. *Cost and Performance Baseline for Fossil Energy Plants Volume 1: Bituminous Coal and Natural Gas to Electricity*; United States, 2022; p Medium: ED, DOI 10.2172/1893822.
49. AspenTech Aspen Plus®. https://www.aspentech.com/en/products/engineering/aspen-plus (accessed 8 November 2023).
50. Ii, M. A. I.; Irvin, N.; Hirata, T.; Nagayasu, H.; Kamijo, T.; Kubota, Y.; Tsujiuchi, T.; Yonekawa, T.; Wood, P., Project Status and Research Plans of 500 TPD CO2 Capture and Sequestration Demonstration at Alabama Power's Plant Barry. *Energy Procedia* **2013,** *37*, 6335-6347, DOI 10.1016/j.egypro.2013.06.563.
51. Bonalumi, D.; Lillia, S.; Valenti, G., Rate-based simulation and techno-economic analysis of coal-fired power plants with aqueous ammonia carbon capture. *Energy Conversion and Management* **2019,** *199*, 111966, DOI 10.1016/j.enconman.2019.111966.
52. Standardization, I. O. f. ISO 14040:2006 Environmental management — Life cycle assessment — Principles and framework. https://www.iso.org/standard/37456.html (accessed 3 November 2023).
53. Standardization, I. O. f. ISO 14044:2006 Environmental management — Life cycle assessment — Requirements and guidelines. https://www.iso.org/standard/38498.html (accessed 3 November 2023).
54. Sphera LCA for Experts (GaBi). https://sphera.com/life-cycle-assessment-lca-software/ (accessed 8 November 2023).
55. Singapore, E. M. A. o. Electricity Generation Fuel Mix. https://www.ema.gov.sg/resources/singapore-energy-statistics/chapter2 (accessed 8 November 2023).
56. ecoinvent ecoinvent v3.9.1. https://ecoinvent.org/the-ecoinvent-database/data-releases/ecoinvent-3-9-1/ (accessed 8 November 2023).
57. Tan, R. B. H.; Wijaya, D.; Khoo, H. H., LCI (Life cycle inventory) analysis of fuels and electricity generation in Singapore. *Energy* **2010,** *35* (12), 4910-4916, DOI 10.1016/j.energy.2010.08.036.
58. Chisalita, D.-A.; Petrescu, L.; Cobden, P.; van Dijk, H. A. J.; Cormos, A.-M.; Cormos, C.-C., Assessing the environmental impact of an integrated steel mill with post-combustion CO2 capture and storage using the LCA methodology. *Journal of Cleaner Production* **2019,** *211*, 1015-1025, DOI 10.1016/j.jclepro.2018.11.256.
59. Giordano, L.; Roizard, D.; Favre, E., Life cycle assessment of post-combustion CO 2 capture: A comparison between membrane separation and chemical absorption processes. *International Journal of Greenhouse Gas Control* **2018,** *68*, 146-163, DOI 10.1016/j.ijggc.2017.11.008.
60. Zakuciová, K.; Kočí, V.; Ciahotný, K.; Carvalho, A.; Štefanica, J.; Smutná, J., Life Cycle Assessment of calcium carbonate loop CO2 capture technology for brown coal power plant unit of the Czech Republic. In *Computer Aided Chemical Engineering*, Friedl, A.; Klemeš, J. J.; Radl, S.; Varbanov, P. S.; Wallek, T., Eds. Elsevier: 2018; Vol. 43, pp 253-258.
61. Guinee, J. B., Handbook on life cycle assessment operational guide to the ISO standards. *The International Journal of Life Cycle Assessment* **2002,** *7* (5), 311-313, DOI 10.1007/BF02978897.
62. Ecology, C.-D. o. I. CML-IA Characterisation Factors. https://www.universiteitleiden.nl/en/research/research-output/science/cml-ia-characterisation-factors (accessed 9 November 2023).
63. Ang, P.; Mothe, S. R.; Chennamaneni, L. R.; Aidil, F.; Khoo, H. H.; Thoniyot, P., Laboratory-Scale Life-Cycle Assessment: A Comparison of Existing and Emerging Methods of Poly(ε-caprolactone) Synthesis. *ACS Sustainable Chemistry & Engineering* **2020,** *9* (2), 669-683, DOI 10.1021/acssuschemeng.0c06247.

64. Heijungs, R.; Huijbregts, M. A. J. In *A review of approaches to treat uncertainty in LCA*, 2004.
65. Henriksson, P. J. G.; Guinée, J. B.; Heijungs, R.; de Koning, A.; Green, D. M., A protocol for horizontal averaging of unit process data—including estimates for uncertainty. *The International Journal of Life Cycle Assessment* **2014,** *19* (2), 429-436, DOI 10.1007/s11367-013-0647-4.
66. Kleijnen, J. P. C., Sensitivity Analysis Versus Uncertainty Analysis: When to Use What? In *Predictability and Nonlinear Modelling in Natural Sciences and Economics*, Grasman, J.; van Straten, G., Eds. Springer Netherlands: Dordrecht, 1994; pp 322-333, DOI 10.1007/978-94-011-0962-8_27.
67. Björklund, A. E., Survey of approaches to improve reliability in lca. *The International Journal of Life Cycle Assessment* **2002,** *7* (2), 64-72, DOI 10.1007/BF02978849.
68. Huijbregts, M., Uncertainty and variability in environmental life-cycle assessment. *The International Journal of Life Cycle Assessment* **2002,** *7* (3), 173-173, DOI 10.1007/BF02994052.
69. Pesonen, H. L.; Ekvall, T.; Fleischer, G.; Huppes, G.; Jahn, C.; Klos, Z. S.; Rebitzer, G.; Sonnemann, G. W.; Tintinelli, A.; Weidema, B. P.; Wenzel, H., Framework for scenario development in LCA. *The International Journal of Life Cycle Assessment* **2000,** *5* (1), 21-30, DOI 10.1007/BF02978555.

For Table of Contents Only

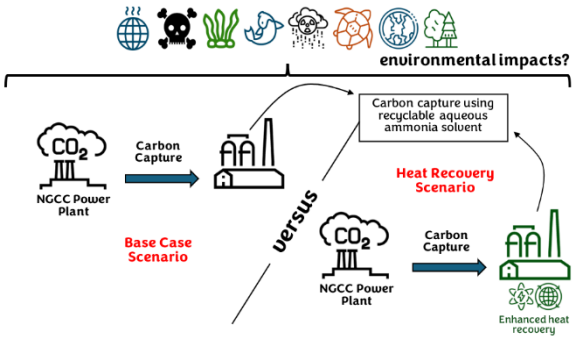

LCA evaluates carbon capture environmental impacts from NGCC power plants using recyclable aqueous ammonia in base and heat recovery scenarios.